



# VTEM™ Plus

---

REPORT ON A HELICOPTER-BORNE VERSATILE TIME  
DOMAIN ELECTROMAGNETIC (VTEM™ Plus) AND HORIZONTAL  
MAGNETIC GRADIOMETER GEOPHYSICAL SURVEY

February 2022

PROJECT: FARWELL GOLD COPPER PROJECT  
LOCATION: WAWA, ON  
FOR: BOLD VENTURES INC.  
SURVEY FLOWN: OCTOBER 2021 – JANUARY 2022  
PROJECT: GL210203

Geotech Ltd.  
270 Industrial Parkway South  
Aurora, ON Canada L4G 3T9

Tel: +1 905 841 5004  
Web: [www.geotech.ca](http://www.geotech.ca)  
Email: [info@geotech.ca](mailto:info@geotech.ca)



# TABLE OF CONTENTS

EXECUTIVE SUMMARY.....	3
1. INTRODUCTION .....	4
1.1 General Considerations.....	4
1.2 Survey And System Specifications .....	5
1.3 Topographic Relief And Cultural Features .....	6
2. DATA ACQUISITION .....	7
2.1 Survey Area.....	7
2.2 Survey Operations .....	7
2.3 Flight Specifications .....	8
2.4 Aircraft and Equipment.....	9
2.4.1 Survey Aircraft .....	9
2.4.2 Electromagnetic System.....	9
2.4.3 Full Waveform VTEM™ Sensor Calibration .....	12
2.4.4 Horizontal Magnetic Gradiometer .....	13
2.4.5 Radar Altimeter .....	13
2.4.6 GPS Navigation System.....	13
2.4.7 Digital Acquisition System .....	13
2.5 Base Station .....	14
3. PERSONNEL .....	15
4. DATA PROCESSING AND PRESENTATION .....	16
4.1 Flight Path.....	16
4.2 Electromagnetic Data .....	16
4.3 Horizontal Magnetic Gradiometer Data.....	18
5. DELIVERABLES.....	19
5.1 Survey Report .....	19
5.2 Maps .....	19
5.3 Digital Data .....	20
6. CONCLUSIONS AND RECOMMENDATIONS .....	24

## LIST OF FIGURES

Figure 1: Survey location .....	4
Figure 2: Survey area location map on Google Earth. ....	5
Figure 3: Farwell Gold Copper Project flight paths over a Google Earth Image.....	6
Figure 4: VTEM™ Transmitter Current Waveform.....	9
Figure 5: VTEM™plus System Configuration. ....	12
Figure 6: Z, X and Fraser filtered X (FFx) components for "thin" target. ....	17

## LIST OF TABLES

Table 1: Survey Specifications.....	7
Table 2: Off-Time Decay Sampling Scheme .....	10
Table 3: VTEM™ System Specifications .....	11
Table 4: Acquisition Sampling Rates .....	13
Table 5: Geosoft GDB Data Format.....	20
Table 6: Geosoft Resistivity Depth Image GDB Data Format .....	22
Table 7: Geosoft database for the VTEM waveform.....	23

## APPENDICES

<b>A.</b> Survey Location Maps.....	A1
<b>B.</b> Survey Area Coordinates .....	B1
<b>C.</b> Geophysical Maps .....	C1
<b>D.</b> Generalized Modelling Results of the VTEM System.....	D1
<b>E.</b> Tau Analysis.....	E1
<b>F.</b> TEM Resistivity Depth Imaging (RDI).....	F1
<b>G.</b> Resistivity Depth Images (RDI) .....	G1

## EXECUTIVE SUMMARY

### FARWELL GOLD COPPER PROJECT WAWA, ON

Between October 27<sup>th</sup>, 2021, to January 11<sup>th</sup>, 2022, Geotech Ltd. carried out a helicopter-borne geophysical survey over the Farwell Gold Copper Project northeast of Wawa, ON.

Principal geophysical sensors included a versatile time domain electromagnetic (VTEM™ Plus) system and a horizontal magnetic gradiometer with two caesium sensors. Ancillary equipment included a GPS navigation system and a radar altimeter. A total of 571 line-kilometres of geophysical data were acquired during the survey.

In-field data quality assurance and preliminary processing were carried out on a daily basis during the acquisition phase. Preliminary and final data processing, including generation of final digital data and map products were undertaken from the office of Geotech Ltd. in Aurora, Ontario.

The final processed survey results are presented as the following maps:

- Electromagnetic stacked profiles of the B-field Z Component
- Electromagnetic stacked profiles of dB/dt Z Component
- B-Field Z Component Channel grid
- dB/dt Z Component Channel grid
- Fraser Filtered X Component Channel grid
- Total Magnetic Intensity (TMI)
- Calculated Time Constant (Tau) with Calculated Vertical Derivative of TMI contours
- Calculated Vertical Gradient (CVG)
- Total Magnetic Horizontal Gradient (TotHG)
- Magnetic Tilt-Angle Derivative (TiltDrv)
- Resistivity Depth Imaging (RDI) sections and depth-slices are presented.

Digital data include all electromagnetic and magnetic products, plus ancillary data including the waveform.

The survey report describes the procedures for data acquisition, equipment used, processing, final image presentation and the specifications for the digital data set.

# 1. INTRODUCTION

## 1.1 GENERAL CONSIDERATIONS

Geotech Ltd. performed a helicopter-borne geophysical survey over the Farwell Gold Copper Project near Wawa, ON (Figure 1 & Figure 2).

David Graham represented Bold Ventures Inc. during the data acquisition and data processing phases of this project.

The geophysical surveys consisted of helicopter borne EM using the versatile time-domain electromagnetic (VTEM™) plus system with Full-Waveform processing. Measurements consisted of Vertical (Z), In-line, and Cross-line Horizontal (X&Y) components of the EM fields using an induction coil and a horizontal magnetic gradiometer using two caesium magnetometers. A total of 571 line-km of geophysical data were acquired during the survey.

The crew was based out of Wawa, ON for the acquisition phase of the survey. Survey flying occurred on November 7<sup>th</sup>, 2021, to January 10<sup>th</sup>, 2022.

Data quality control and quality assurance, and preliminary data processing were carried out on a daily basis during the acquisition phase of the project. Final data processing followed immediately after the end of survey. Final reporting, data presentation, and archiving was completed in February 2022.

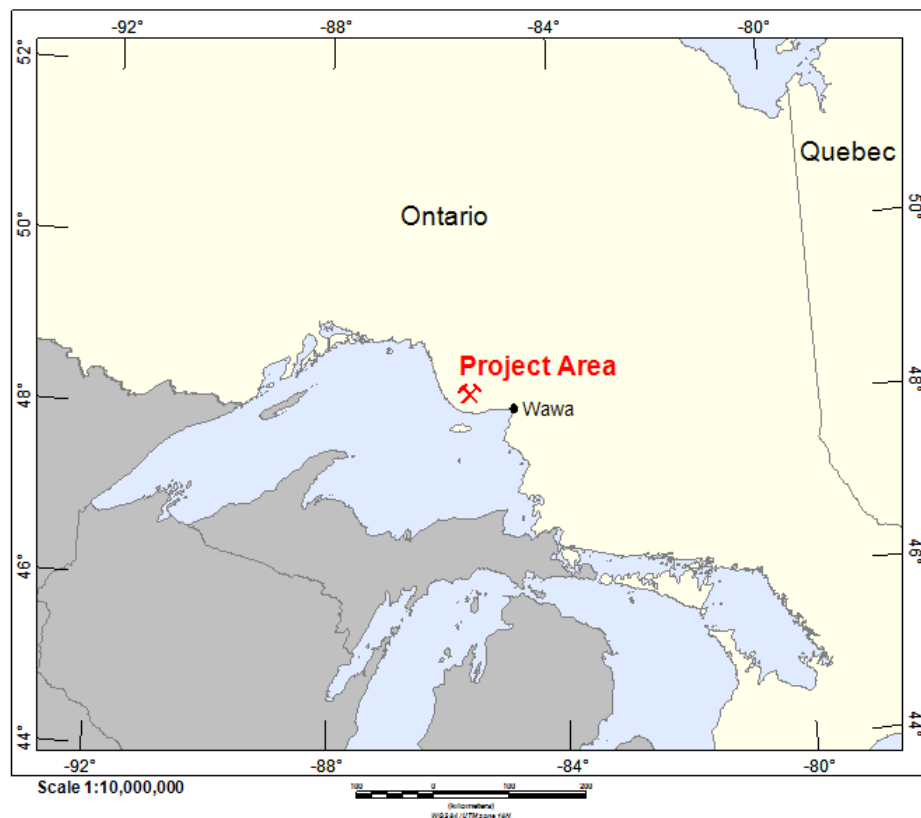


Figure 1: Survey location

## 1.2 SURVEY AND SYSTEM SPECIFICATIONS

The survey area is located approximately 56km northwest of Wawa, ON (Figure 2).

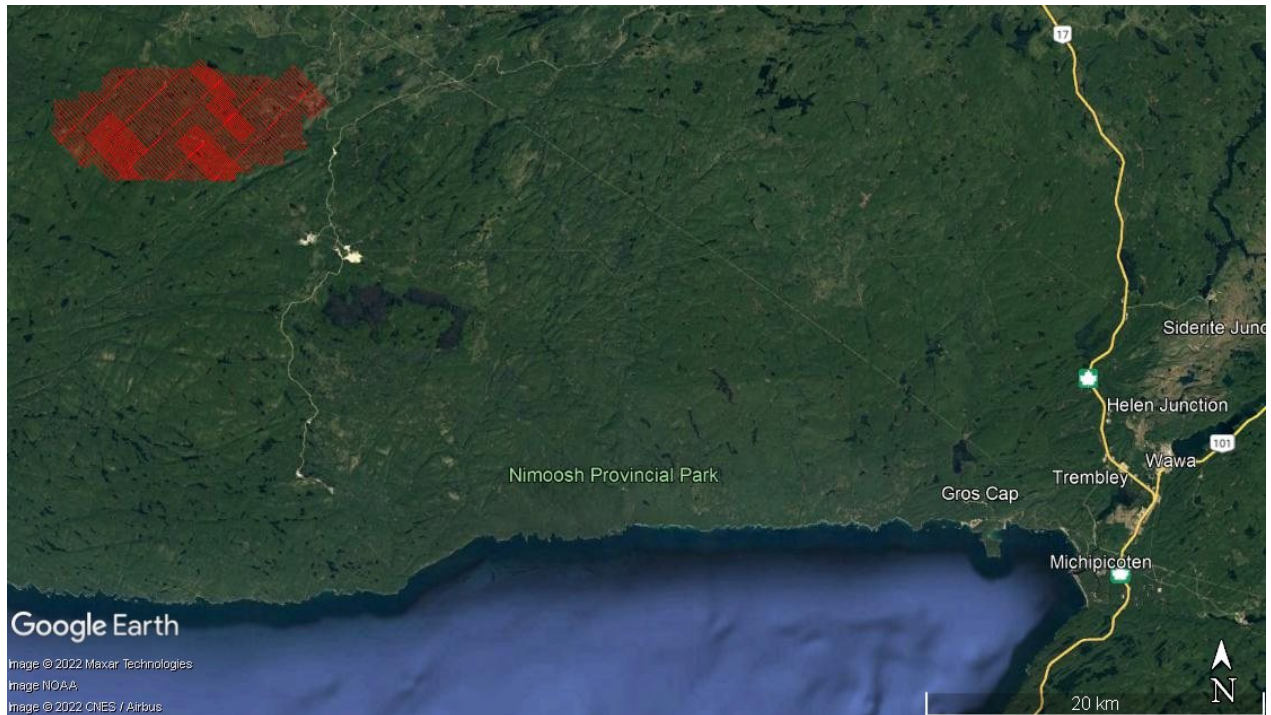


Figure 2: Survey area location map on Google Earth.

The Farwell Gold Copper Project was flown in a northwest to southeast (N 135° E azimuth) direction with traverse line spacings of 100 - 200 metres, as depicted in Figure 3. Tie lines were flown perpendicular to traverse lines at 2000m line spacing. For more detailed information on the flight spacings and directions, see Table 1.

### 1.3 TOPOGRAPHIC RELIEF AND CULTURAL FEATURES

Topographically, the survey area exhibits relief with elevations ranging from 353 to 593 metres over an area of 86 square kilometres (Figure 3).

There are visible signs of culture such as roads/trails within the Farwell Gold Copper Project area.



Figure 3: Farwell Gold Copper Project flight paths over a Google Earth Image.

## 2. DATA ACQUISITION

### 2.1 SURVEY AREA

The survey area (see Figure 3 and Appendix A) and general flight specifications are as follows:

**Table 1:** Survey Specifications

Survey block	Line spacing (m)	Area (Km <sup>2</sup> )	Planned Line-km	Actual <sup>1</sup> Line-km	Flight direction	Line numbers
Farwell Gold Copper	Traverse: 100 - 200	86	556	571	N135°E / N315°E	L1000 – L1650
	Tie: 2000				N45°E / N225°E	T3000 – T3040
TOTAL		86	556	571		

Survey area boundaries co-ordinates are provided in Appendix B.

### 2.2 SURVEY OPERATIONS

Survey operations were based out of Wawa, ON. The following table shows the timing of the flying.

Date	Comments
27-Oct	Mobilization
28-Oct	System assembly
29-Oct	System assembly, set up base stations
30-Oct	Helicopter installation
31-Oct	Weather day
01-Nov	System tests
02-Nov	Helicopter maintenance
03-Nov	Helicopter maintenance
04-Nov	Helicopter maintenance
05-Nov	Helicopter maintenance
06-Nov	Weather day
07-Nov	Production Flight - 130 km flown
08-Nov	Crew change
09-Nov	Production Flight - 8 km flown
10-Nov	Production Flight - 80 km flown
11-Nov	Standby
12-Nov	Standby
13-Nov	Weather day
14-Nov	Weather day
15-Nov	Weather day
16-Nov	Production Flight - 20 km flown
17-Nov	Weather day
18-Nov	Weather day

<sup>1</sup> Note: Actual Line kilometres represent the total line kilometres in the final database. These line-km normally exceed the Planned Line-km, as indicated in the survey NAV files. This survey was shut down for the holidays and will resume in the new year.



Date	Comments
19-Nov	Production Flight - 104 km flown
20-Nov	Weather day
21-Nov	Weather day
22-Nov	Weather day
23-Nov	Weather day
24-Nov	Weather day
25-Nov	Weather day
26-Nov	Weather day
27-Nov	Production Flight - 58 km flown
28-Nov	Standby for replacement helicopter
29-Nov	Standby for replacement helicopter
30-Nov	Standby for replacement helicopter
01-Dec	Standby for replacement helicopter
02-Dec	Standby for replacement helicopter
03-Dec	Helicopter installation
04-Dec	Helicopter installation
05-Dec	Calibration and tests
06-Dec	System repairs
07-Dec	System repairs
08-Dec	System repairs
09-Dec	Weather day
10-Dec	Production Flight - 41 km flown
11-Dec	Weather day
12-Dec	Weather day
13-Dec	Production Flight - 32 km flown
14-Dec	Production Flight - 23 km flown
15-Dec	Weather day
16-Dec	Weather day
17-Dec	Weather day
18-Dec	Helicopter installation completed
19-Dec	Radar and calibration tests
20-Dec	Demobilization
	Break for the Holidays
06-Jan	Mobilization
07-Jan	Set up system, base station. Production Flight – 40 km flown
08-Jan	Weather Day
09-Jan	Technical Issues & troubleshooting
10-Jan	Production Flight – 28 km flown. Flight path completed
11-Jan	Demobilization

### 2.3 FLIGHT SPECIFICATIONS

During the survey, the helicopter was maintained at a mean altitude of 98 metres above the ground with an average survey speed of 80 km/hour. This allowed for an actual average Transmitter-receiver loop terrain clearance of 50 metres and a magnetic sensor clearance of 60 metres.

The on-board operator was responsible for monitoring the system integrity. He also maintained a detailed flight log during the survey, tracking the times of the flight as well as any unusual geophysical or topographic features.

On return of the aircrew to the base camp the survey data was transferred from a compact flash card (PCMCIA) to the data processing computer. The data were then uploaded via ftp to the Geotech office in Aurora for daily quality assurance and quality control by qualified personnel.

## 2.4 AIRCRAFT AND EQUIPMENT

### 2.4.1 SURVEY AIRCRAFT

The survey was flown using Eurocopter Aerospatiale (A-Star) 350 B3 helicopters, registration C-GVMU, C-GEOC, and C-GLHX. The helicopters are owned and operated by Geotech Aviation Ltd. Installation of the geophysical and ancillary equipment was carried out by a Geotech Ltd. crew.

### 2.4.2 ELECTROMAGNETIC SYSTEM

The electromagnetic system was a Geotech Time Domain EM (VTEM™ Plus) full receiver-waveform streamed data recorded system. The “full waveform VTEM system” uses the streamed half-cycle recording of transmitter and receiver waveforms to obtain a complete system response calibration throughout the entire survey flight. VTEM with the serial number 10 had been used for the survey. The VTEM™ transmitter current waveform is shown diagrammatically in Figure 4.

The VTEM™ Receiver and transmitter coils were in concentric-coplanar and Z-direction oriented configuration. The receiver system for the project also included coincident-coaxial X&Y-direction coils to measure the in-line and cross-line dB/dt and calculate B-Field responses. The Transmitter-receiver loop was towed at a mean distance of 48 metres below the aircraft as shown in Figure 5.

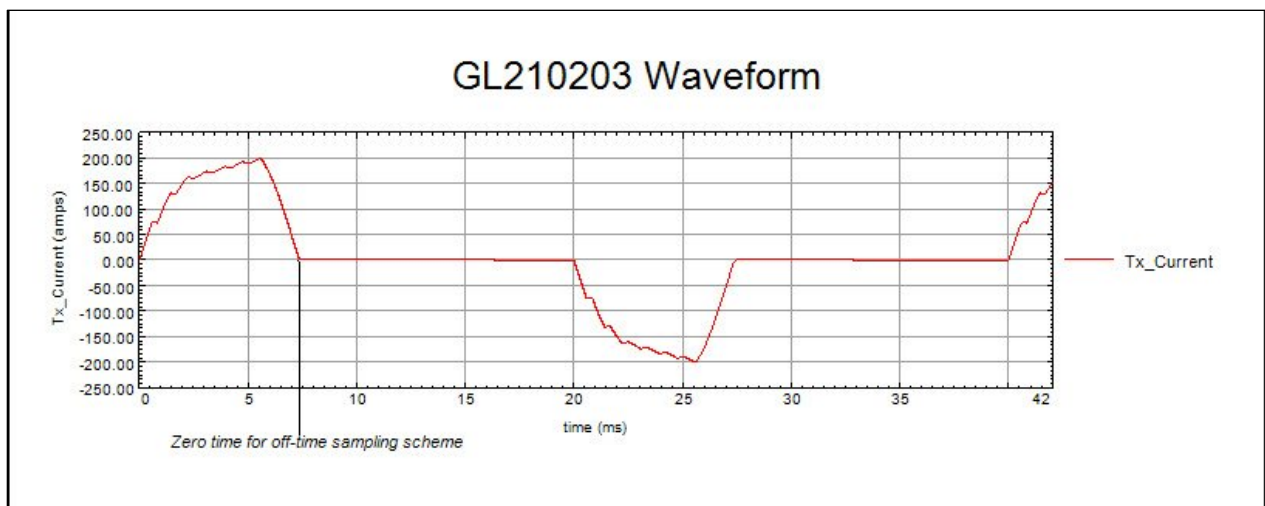


Figure 4: VTEM™ Transmitter Current Waveform

The VTEM™ decay sampling scheme is shown in Table 2 below. Forty-three-time measurement gates were used for the final data processing in the range from 0.021 to 8.083 msec. Zero time for the off-time sampling scheme is equal to the current pulse width and is defined as the time near the end of the turn-off ramp where the dI/dt waveform falls to 1/2 of its peak value.

**Table 2:** Off-Time Decay Sampling Scheme

VTEM™ Decay Sampling Scheme				
Index	Start	End	Middle	Width
Milliseconds				
4	0.018	0.023	0.021	0.005
5	0.023	0.029	0.026	0.005
6	0.029	0.034	0.031	0.005
7	0.034	0.039	0.036	0.005
8	0.039	0.045	0.042	0.006
9	0.045	0.051	0.048	0.007
10	0.051	0.059	0.055	0.008
11	0.059	0.068	0.063	0.009
12	0.068	0.078	0.073	0.010
13	0.078	0.090	0.083	0.012
14	0.090	0.103	0.096	0.013
15	0.103	0.118	0.110	0.015
16	0.118	0.136	0.126	0.018
17	0.136	0.156	0.145	0.020
18	0.156	0.179	0.167	0.023
19	0.179	0.206	0.192	0.027
20	0.206	0.236	0.220	0.030
21	0.236	0.271	0.253	0.035
22	0.271	0.312	0.290	0.040
23	0.312	0.358	0.333	0.046
24	0.358	0.411	0.383	0.053
25	0.411	0.472	0.440	0.061
26	0.472	0.543	0.505	0.070
27	0.543	0.623	0.580	0.081
28	0.623	0.716	0.667	0.093
29	0.716	0.823	0.766	0.107
30	0.823	0.945	0.880	0.122
31	0.945	1.086	1.010	0.141
32	1.086	1.247	1.161	0.161
33	1.247	1.432	1.333	0.185
34	1.432	1.646	1.531	0.214
35	1.646	1.891	1.760	0.245
36	1.891	2.172	2.021	0.281
37	2.172	2.495	2.323	0.323
38	2.495	2.865	2.667	0.370

VTEM™ Decay Sampling Scheme				
Index	Start	End	Middle	Width
Milliseconds				
39	2.865	3.292	3.063	0.427
40	3.292	3.781	3.521	0.490
41	3.781	4.341	4.042	0.560
42	4.341	4.987	4.641	0.646
43	4.987	5.729	5.333	0.742
44	5.729	6.581	6.125	0.852
45	6.581	7.560	7.036	0.979
46	7.560	8.685	8.083	1.125

Z Component: 4-46 time gates  
X Component: 20-46 time gates  
Y Component: 20-46 time gates

**Table 3:** VTEM™ System Specifications

Transmitter	Receiver
<ul style="list-style-type: none"> <li>• Transmitter loop diameter: 26 m</li> <li>• Number of turns: 4</li> <li>• Effective Transmitter loop area: 2123.7 m<sup>2</sup></li> <li>• Transmitter base frequency: 30 Hz</li> <li>• Peak current: 199.9 A</li> <li>• Pulse width: 7.36 ms</li> <li>• Waveform shape: Bi-polar trapezoid</li> <li>• Peak dipole moment: 424,467 nIA</li> <li>• Average transmitter-receiver loop terrain clearance: 50 metres</li> </ul>	<ul style="list-style-type: none"> <li>• X -Coil diameter: 0.32 m</li> <li>• Number of turns: 245</li> <li>• Effective coil area: 19.69 m<sup>2</sup></li> <li>• Y -Coil diameter: 0.32 m</li> <li>• Number of turns: 245</li> <li>• Effective coil area: 19.69 m<sup>2</sup></li> <li>• Z-Coil diameter: 1.2 m</li> <li>• Number of turns: 100</li> <li>• Effective coil area: 113.04 m<sup>2</sup></li> </ul>

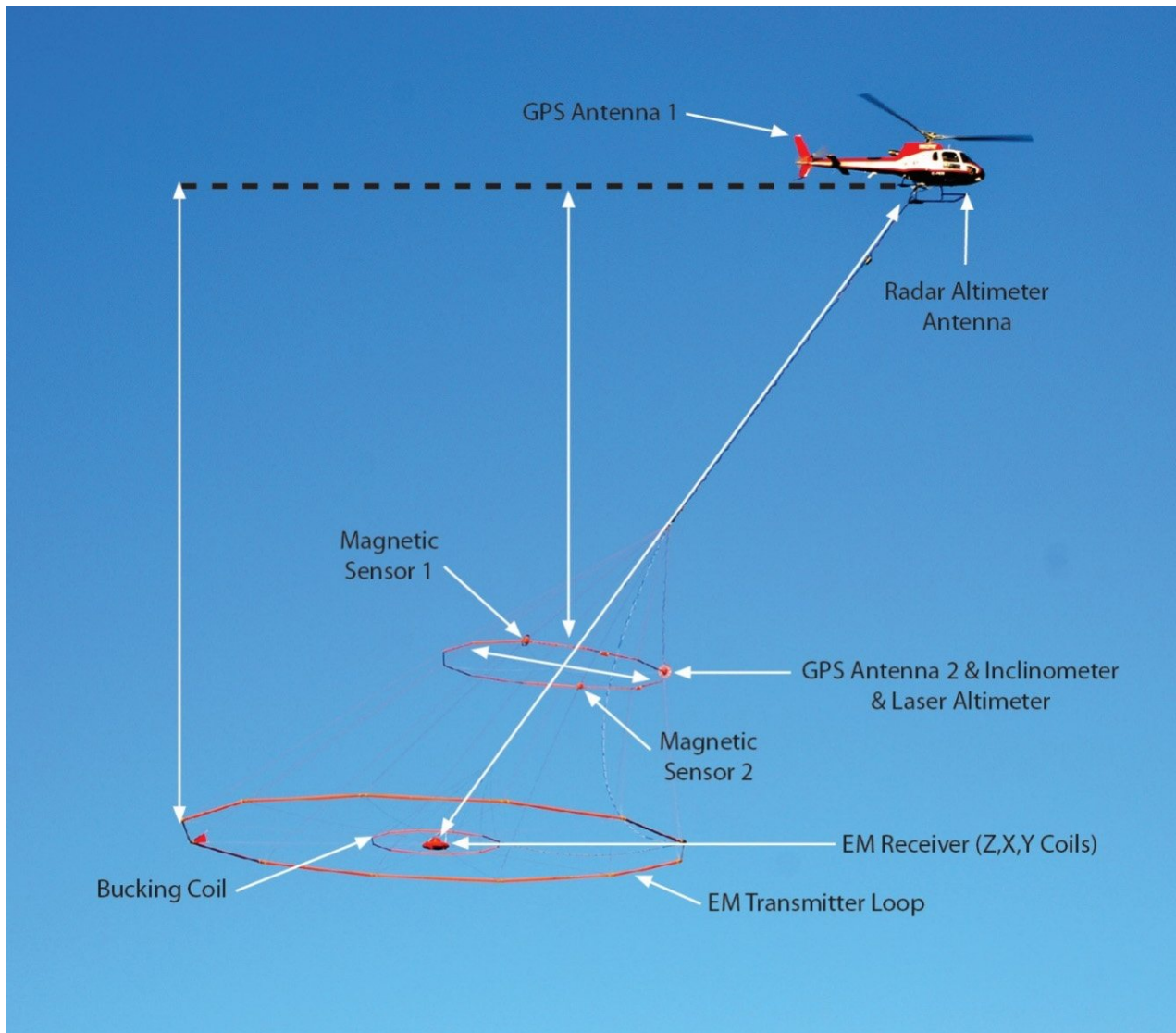


Figure 5: VTEM™plus System Configuration.

### 2.4.3 FULL WAVEFORM VTEM™ SENSOR CALIBRATION

The calibration is performed on the complete VTEM™ system installed in and connected to the helicopter, using special calibration equipment. This calibration takes place on the ground at the start of the project prior to surveying.

The procedure takes half-cycle files acquired and calculates a calibration file consisting of a single stacked half-cycle waveform. The purpose of the stacking is to attenuate natural and man-made magnetic signals, leaving only the response to the calibration signal.

This calibration allows the transfer function between the EM receiver and data acquisition system and the transfer function between the current monitor and data acquisition system to be determined. These calibration results are then used in VTEM full waveform processing.

#### 2.4.4 HORIZONTAL MAGNETIC GRADIOMETER

The horizontal magnetic gradiometer consists of two Geometrics split-beam field magnetic sensors with a sampling interval of 0.1 seconds. These sensors are mounted 12.5 metres apart on a separate loop, 10 metres above the Transmitter-receiver loop. A GPS antenna and Gyro Inclinator is installed on the separate loop to accurately record the tilt and position of the magnetic gradiometer sensors.

#### 2.4.5 RADAR ALTIMETER

A Terra TRA 3000/TRI 40 radar altimeter was used to record terrain clearance. The antenna was mounted beneath the bubble of the helicopter cockpit (Figure 5).

#### 2.4.6 GPS NAVIGATION SYSTEM

The navigation system used was a Geotech PC104 based navigation system utilizing a NovAtel's WAAS(Wide Area Augmentation System) enabled GPS receiver, Geotech navigate software, a full screen display with controls in front of the pilot to direct the flight and a NovAtel GPS antenna mounted on the helicopter tail (Figure 5). As many as 11 GPS and two WAAS satellites may be monitored at any one time. The positional accuracy or circular error probability (CEP) is 1.8 m, with WAAS active, it is 1.0 m. The coordinates of the survey area were set-up prior to the survey and the information was fed into the airborne navigation system. The second GPS antenna is installed on the additional magnetic loop together with Gyro Inclinator.

#### 2.4.7 DIGITAL ACQUISITION SYSTEM

A Geotech data acquisition system recorded the digital survey data on an internal compact flash card. Data is displayed on an LCD screen as traces to allow the operator to monitor the integrity of the system. The data type and sampling interval as provided in Table 4

Table 4: Acquisition Sampling Rates

Data Type	Sampling
TDEM	0.1 sec
Magnetometer	0.1 sec
GPS Position	0.2 sec
Radar Altimeter	0.2 sec
Inclinometer	0.1 sec

## 2.5 BASE STATION

A combined magnetometer/GPS base station was utilized on this project. A Geometrics Caesium vapour magnetometer was used as a magnetic sensor with a sensitivity of 0.001 nT. The base station was recording the magnetic field together with the GPS time at 1 Hz on a base station computer.

The base station magnetometer sensor was installed in a secured location away from electric transmission lines and moving ferrous objects such as motor vehicles. The base station data were backed-up to the data processing computer at the end of each survey day.

### 3. PERSONNEL

The following Geotech Ltd. personnel were involved in the project.

#### FIELD:

Project Manager: Steven Cargnello (Office)

Data QC: Nick Venter

Crew chief: Paul Taylor  
Rafael Coyoli

Operator: Jan Dabrowski

The survey pilot and the mechanical engineer were employed directly by the helicopter operator – Geotech Aviation Ltd.

Pilot: Rob Girard  
Alexander Cyr  
Ian McGreer

Mechanical Engineer: Stephen McGreer

#### OFFICE:

Preliminary Data Processing: Matthew Johnson  
Nick Venter

Final Data Processing: Mike Finlayson

Data QA/QC: TaiChyi Shei  
Jean Legault

Reporting/Mapping: Emily Data

Processing and Interpretation phases were carried out under the supervision of TaiChyi Shei & Jean M. Legault, Chief Geophysicist. The customer relations were looked after by Paolo Berardelli.



## 4. DATA PROCESSING AND PRESENTATION

Data compilation and processing were carried out by the application of Geosoft OASIS Montaj and programs proprietary to Geotech Ltd.

### 4.1 FLIGHT PATH

The flight path, recorded by the acquisition program as WGS 84 latitude/longitude, was converted into the WGS84 Datum, UTM Zone 16N coordinate system in Oasis Montaj.

The flight path was drawn using linear interpolation between x, y positions from the navigation system. Positions are updated every second and expressed as UTM easting's (x) and UTM northing's (y).

### 4.2 ELECTROMAGNETIC DATA

The Full Waveform EM specific data processing operations included:

- Half cycle stacking (performed at time of acquisition).
- System response correction.
- Parasitic and drift removal.

A three-stage digital filtering process was used to reject major spheric events and to reduce noise levels. Local spheric activity can produce sharp, large amplitude events that cannot be removed by conventional filtering procedures. Smoothing or stacking will reduce their amplitude but leave a broader residual response that can be confused with geological phenomena. To avoid this possibility, a computer algorithm searches out and rejects the major spheric events.

The signal to noise ratio was further improved by the application of a low pass linear digital filter. This filter has zero phase shift which prevents any lag or peak displacement from occurring, and it suppresses only variations with a wavelength less than about 1 second or 15 metres. This filter is a symmetrical 1 sec linear filter.

The results are presented as stacked profiles of EM voltages for the time gates, in linear - logarithmic scale for the B-field Z component and dB/dt responses in the Z and X components. B-field Z component time channels recorded at 0.7660 milliseconds after the termination of the impulse is also presented as a colour image. Calculated Time Constant (TAU) with Calculated Vertical Derivative contours is presented in Appendix C. Resistivity Depth Image (RDI) is also presented in Appendix G.

VTEM™ has three receiver coil orientations. Z-axis coil is oriented parallel to the transmitter coil axis, and both are horizontal to the ground. The X-axis coil is oriented parallel to the ground and along the line-of-flight. The Y-axis coil is oriented parallel to the ground and across the line-of-flight. The combination of the X, Y, and Z coils configuration provides information on the position, depth, dip, and thickness of a conductor. Generalized modeling results of VTEM data are shown in Appendix D.

In general X-component data produce cross-over type anomalies: from “+ to -” in flight direction of flight for “thin” sub vertical targets and from “- to +” in direction of flight for “thick” targets. Z component data produce double peak type anomalies for “thin” sub vertical targets and single peak for “thick” targets. The limits and change-over of “thin-thick” depends on dimensions of a TEM system (Appendix D, Figure D-16).

Because of X component polarity is under line-of-flight, convolution Fraser Filter (Figure 6) is applied to X component data to represent axes of conductors in the form of grid map. In this case positive FF anomalies always correspond to “plus-to-minus” X data crossovers independent of the flight direction.

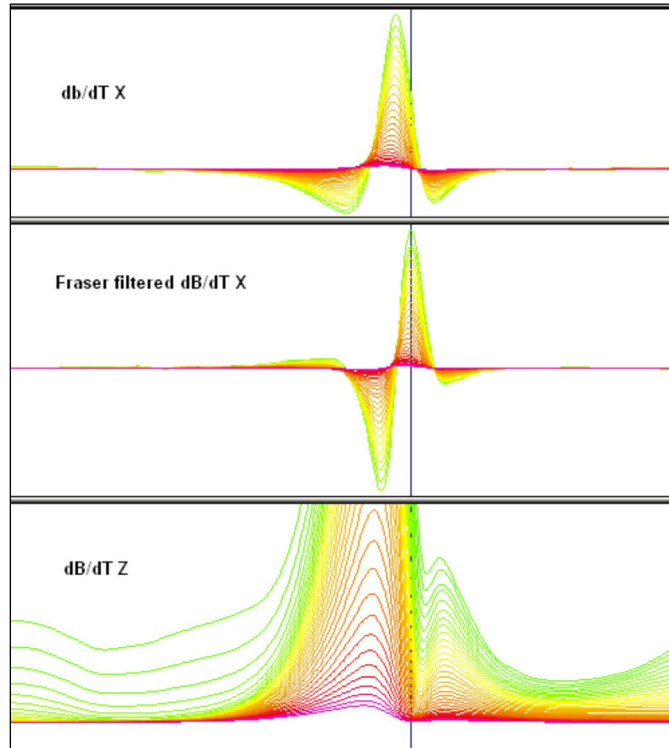


Figure 6: Z, X and Fraser filtered X (FFx) components for “thin” target.

### 4.3 HORIZONTAL MAGNETIC GRADIOMETER DATA

The horizontal gradients data from the VTEM™ Plus are measured by two magnetometers 12.5 m apart on an independent bird mounted 10m above the VTEM™ loop. A GPS and a Gyro Inclinometer help to determine the positions and orientations of the magnetometers. The data from the two magnetometers are corrected for position and orientation variations, as well as for the diurnal variations using the base station data.

The position of the centre of the horizontal magnetic gradiometer bird is calculated from the GPS utilizing in-house processing tool in Geosoft. Following that total magnetic intensity is calculated at the center of the bird by calculating the mean values from both sensors. In addition to the total intensity advanced processing is done to calculate the in-line and crossline (or lateral) horizontal gradient which enhance the understanding of magnetic targets. The in-line (longitudinal) horizontal gradient is calculated from the difference of two consecutive total magnetic field readings divided by the distance along the flight line direction, while the crossline (lateral) horizontal magnetic gradient is calculated from the difference in the magnetic readings from both magnetic sensors divided by their horizontal separation.

Two advanced magnetic derivative products, the total horizontal derivative (THDR), and tilt angle derivative and are also created. The total horizontal derivative or gradient is defined as:

$THDR = \sqrt{H_x^2 + H_y^2}$ , where  $H_x$  and  $H_y$  are crossline and in-line horizontal gradients.

The tilt angle derivative (TDR) is defined as:

$TDR = \arctan (V_z/THDR)$ , where THDR is the total horizontal derivative, and  $V_z$  is the vertical derivative.

Measured crossline gradients can help to enhance crossline linear features during gridding.

## 5. DELIVERABLES

### 5.1 SURVEY REPORT

The survey report describes the data acquisition, processing, and final presentation of the survey results. The survey report is provided in two paper copies and digitally in PDF format.

### 5.2 MAPS

Final maps were produced at scale of 1:15,000 for best representation of the survey size and line spacing. The coordinate/projection system used was WGS84 Datum, UTM Zone 16N. All maps show the flight path trace and topographic data; latitude and longitude are also noted on maps.

The results of the survey are presented as EM profiles, a late-time gate gridded EM channel, and a colour magnetic TMI contour map.

- Maps at 1:15,000 in Geosoft MAP format, as follows:

GL210203_15k_dBdt:	dB/dt profiles Z Component, Time Gates 0.220 – 7.036 ms in linear – logarithmic scale.
GL210203_15k_BField:	B-field profiles Z Component, Time Gates 0.220 – 7.036 ms in linear – logarithmic scale.
GL210203_15k_BFz29:	B-field Z Component Channel 29, Time Gate 0.7660 ms colour image.
GL210203_15k_SFz29:	VTEM dB/dt Z Component Channel 29, Time Gate 0.7660 ms colour image
GL210203_15k_SFxFF26:	Fraser Filtered dB/dt X Component Channel 26, Time Gate 0.505 ms colour image.
GL210203_15k_TauSF:	dB/dt Calculated Time Constant (Tau) with Calculated Vertical Derivative contours
GL210203_15k_TMI:	Total Magnetic Intensity (TMI) colour image and contours.
GL210203_15k_CVG:	Calculated Vertical Derivative (nT/m)
GL210203_15k_TotHG:	Magnetic Total Horizontal Gradient (nT/m)
GL210203_15k_TiltDrv:	Magnetic Tilt Derivative (radians)

- Maps are also presented in PDF format.
- The topographic data base was derived from 1:50,000 CANVEC data. Background shading is from ASTER GDEM (<https://gdex.cr.usgs.gov/gdex>). Inset data derived from the Geocommunities ([www.geocomm.com](http://www.geocomm.com))
- A Google Earth file *GL210203\_Bold\_Prelim.kmz* showing the flight path of the block is included. Free versions of Google Earth software from: <http://earth.google.com/download-earth.html>

### 5.3 DIGITAL DATA

Two copies of the data and maps on DVD were prepared to accompany the report. Each DVD contains a digital file of the line data in GDB Geosoft Montaj format as well as the maps in Geosoft Montaj Map and PDF format.

- DVD structure.

Data contains databases, grids and maps, as described below.  
 Report contains a copy of the report and appendices in PDF format.

Databases in Geosoft GDB format, containing the channels listed in Table 5.

**Table 5:** Geosoft GDB Data Format

Channel name	Units	Description
X	metres	Easting WGS84 Zone 16N
Y	metres	Northing WGS84 Zone 16N
Longitude	Decimal Degrees	WGS84 Longitude data
Latitude	Decimal Degrees	WGS84 Latitude data
Z	metres	GPS antenna elevation
Zb	metres	EM bird elevation
Radar	metres	Helicopter terrain clearance from radar altimeter
Radarb	metres	Calculated EM transmitter-receiver loop terrain clearance from radar altimeter
DEM	metres	Digital Elevation Model
Gtime	Seconds of the day	GPS time
Mag1L	nT	Measured Total Magnetic Field data (left sensor)
Mag1R	nT	Measured Total Magnetic Field data (right sensor)
Mag2LZ	nT	Z corrected (w.r.t. loop center) and diurnal corrected magnetic field left mag
Mag2RZ	nT	Z corrected (w.r.t. loop center) and diurnal corrected magnetic field right mag
Basemag	nT	Magnetic diurnal variation data
TMI2	nT	Calculated from diurnal corrected total magnetic field intensity of the centre of the loop
TMI3	nT	Microleveled total magnetic field intensity of the centre of the loop
Hginline		Calculated in-line gradient
Hgcxline		Measured cross-line gradient
CVG	nT/m	Calculated Magnetic Vertical Gradient of TMI
SFz[4]	pV/(A*m <sup>4</sup> )	Z dB/dt 0.021 millisecond time channel
SFz[5]	pV/(A*m <sup>4</sup> )	Z dB/dt 0.026 millisecond time channel
SFz[6]	pV/(A*m <sup>4</sup> )	Z dB/dt 0.031 millisecond time channel
SFz[7]	pV/(A*m <sup>4</sup> )	Z dB/dt 0.036 millisecond time channel
SFz[8]	pV/(A*m <sup>4</sup> )	Z dB/dt 0.042 millisecond time channel
SFz[9]	pV/(A*m <sup>4</sup> )	Z dB/dt 0.048 millisecond time channel
SFz[10]	pV/(A*m <sup>4</sup> )	Z dB/dt 0.055 millisecond time channel
SFz[11]	pV/(A*m <sup>4</sup> )	Z dB/dt 0.063 millisecond time channel
SFz[12]	pV/(A*m <sup>4</sup> )	Z dB/dt 0.073 millisecond time channel
SFz[13]	pV/(A*m <sup>4</sup> )	Z dB/dt 0.083 millisecond time channel
SFz[14]	pV/(A*m <sup>4</sup> )	Z dB/dt 0.096 millisecond time channel

Channel name	Units	Description
SFz[15]	pV/(A*m <sup>4</sup> )	Z dB/dt 0.110 millisecond time channel
SFz[16]	pV/(A*m <sup>4</sup> )	Z dB/dt 0.126 millisecond time channel
SFz[17]	pV/(A*m <sup>4</sup> )	Z dB/dt 0.145 millisecond time channel
SFz[18]	pV/(A*m <sup>4</sup> )	Z dB/dt 0.167 millisecond time channel
SFz[19]	pV/(A*m <sup>4</sup> )	Z dB/dt 0.192 millisecond time channel
SFz[20]	pV/(A*m <sup>4</sup> )	Z dB/dt 0.220 millisecond time channel
SFz[21]	pV/(A*m <sup>4</sup> )	Z dB/dt 0.253 millisecond time channel
SFz[22]	pV/(A*m <sup>4</sup> )	Z dB/dt 0.290 millisecond time channel
SFz[23]	pV/(A*m <sup>4</sup> )	Z dB/dt 0.333 millisecond time channel
SFz[24]	pV/(A*m <sup>4</sup> )	Z dB/dt 0.383 millisecond time channel
SFz[25]	pV/(A*m <sup>4</sup> )	Z dB/dt 0.440 millisecond time channel
SFz[26]	pV/(A*m <sup>4</sup> )	Z dB/dt 0.505 millisecond time channel
SFz[27]	pV/(A*m <sup>4</sup> )	Z dB/dt 0.580 millisecond time channel
SFz[28]	pV/(A*m <sup>4</sup> )	Z dB/dt 0.667 millisecond time channel
SFz[29]	pV/(A*m <sup>4</sup> )	Z dB/dt 0.766 millisecond time channel
SFz[30]	pV/(A*m <sup>4</sup> )	Z dB/dt 0.880 millisecond time channel
SFz[31]	pV/(A*m <sup>4</sup> )	Z dB/dt 1.010 millisecond time channel
SFz[32]	pV/(A*m <sup>4</sup> )	Z dB/dt 1.161 millisecond time channel
SFz[33]	pV/(A*m <sup>4</sup> )	Z dB/dt 1.333 millisecond time channel
SFz[34]	pV/(A*m <sup>4</sup> )	Z dB/dt 1.531 millisecond time channel
SFz[35]	pV/(A*m <sup>4</sup> )	Z dB/dt 1.760 millisecond time channel
SFz[36]	pV/(A*m <sup>4</sup> )	Z dB/dt 2.021 millisecond time channel
SFz[37]	pV/(A*m <sup>4</sup> )	Z dB/dt 2.323 millisecond time channel
SFz[38]	pV/(A*m <sup>4</sup> )	Z dB/dt 2.667 millisecond time channel
SFz[39]	pV/(A*m <sup>4</sup> )	Z dB/dt 3.063 millisecond time channel
SFz[40]	pV/(A*m <sup>4</sup> )	Z dB/dt 3.521 millisecond time channel
SFz[41]	pV/(A*m <sup>4</sup> )	Z dB/dt 4.042 millisecond time channel
SFz[42]	pV/(A*m <sup>4</sup> )	Z dB/dt 4.641 millisecond time channel
SFz[43]	pV/(A*m <sup>4</sup> )	Z dB/dt 5.333 millisecond time channel
SFz[44]	pV/(A*m <sup>4</sup> )	Z dB/dt 6.125 millisecond time channel
SFz[45]	pV/(A*m <sup>4</sup> )	Z dB/dt 7.036 millisecond time channel
SFz[46]	pV/(A*m <sup>4</sup> )	Z dB/dt 8.083 millisecond time channel
SFx[20]	pV/(A*m <sup>4</sup> )	X dB/dt 0.220 millisecond time channel
SFx[21]	pV/(A*m <sup>4</sup> )	X dB/dt 0.253 millisecond time channel
SFx[22]	pV/(A*m <sup>4</sup> )	X dB/dt 0.290 millisecond time channel
SFx[23]	pV/(A*m <sup>4</sup> )	X dB/dt 0.333 millisecond time channel
SFx[24]	pV/(A*m <sup>4</sup> )	X dB/dt 0.383 millisecond time channel
SFx[25]	pV/(A*m <sup>4</sup> )	X dB/dt 0.440 millisecond time channel
SFx[26]	pV/(A*m <sup>4</sup> )	X dB/dt 0.505 millisecond time channel
SFx[27]	pV/(A*m <sup>4</sup> )	X dB/dt 0.580 millisecond time channel
SFx[28]	pV/(A*m <sup>4</sup> )	X dB/dt 0.667 millisecond time channel
SFx[29]	pV/(A*m <sup>4</sup> )	X dB/dt 0.766 millisecond time channel
SFx[30]	pV/(A*m <sup>4</sup> )	X dB/dt 0.880 millisecond time channel
SFx[31]	pV/(A*m <sup>4</sup> )	X dB/dt 1.010 millisecond time channel
SFx[32]	pV/(A*m <sup>4</sup> )	X dB/dt 1.161 millisecond time channel
SFx[33]	pV/(A*m <sup>4</sup> )	X dB/dt 1.333 millisecond time channel
SFx[34]	pV/(A*m <sup>4</sup> )	X dB/dt 1.531 millisecond time channel
SFx[35]	pV/(A*m <sup>4</sup> )	X dB/dt 1.760 millisecond time channel
SFx[36]	pV/(A*m <sup>4</sup> )	X dB/dt 2.021 millisecond time channel
SFx[37]	pV/(A*m <sup>4</sup> )	X dB/dt 2.323 millisecond time channel

Channel name	Units	Description
SFx[38]	$\text{pV}/(\text{A}\cdot\text{m}^4)$	X dB/dt 2.667 millisecond time channel
SFx[39]	$\text{pV}/(\text{A}\cdot\text{m}^4)$	X dB/dt 3.063 millisecond time channel
SFx[40]	$\text{pV}/(\text{A}\cdot\text{m}^4)$	X dB/dt 3.521 millisecond time channel
SFx[41]	$\text{pV}/(\text{A}\cdot\text{m}^4)$	X dB/dt 4.042 millisecond time channel
SFx[42]	$\text{pV}/(\text{A}\cdot\text{m}^4)$	X dB/dt 4.641 millisecond time channel
SFx[43]	$\text{pV}/(\text{A}\cdot\text{m}^4)$	X dB/dt 5.333 millisecond time channel
SFx[44]	$\text{pV}/(\text{A}\cdot\text{m}^4)$	X dB/dt 6.125 millisecond time channel
SFx[45]	$\text{pV}/(\text{A}\cdot\text{m}^4)$	X dB/dt 7.036 millisecond time channel
SFx[46]	$\text{pV}/(\text{A}\cdot\text{m}^4)$	X dB/dt 8.083 millisecond time channel
SFy	$\text{pV}/(\text{A}\cdot\text{m}^4)$	Y dB/dt data for time channels 20 to 46
BFz	$(\text{pV}\cdot\text{ms})/(\text{A}\cdot\text{m}^4)$	Z B-Field data for time channels 4 to 46
BFx	$(\text{pV}\cdot\text{ms})/(\text{A}\cdot\text{m}^4)$	X B-Field data for time channels 20 to 46
BFy	$(\text{pV}\cdot\text{ms})/(\text{A}\cdot\text{m}^4)$	Y B-Field data for time channels 20 to 46
SFxFF	$\text{pV}/(\text{A}\cdot\text{m}^4)$	Fraser Filtered X dB/dt
NchanBF		Latest time channels of TAU calculation
TauBF	ms	Time constant B-Field
NchanSF		Latest time channels of TAU calculation
TauSF	ms	Time constant dB/dt
PLM		60 Hz power line monitor

Electromagnetic B-field and dB/dt Z component data is found in array channel format between indexes 4 – 46, and X & Y component data from 20 – 46, as described above.

- Database of the Resistivity Depth Images in Geosoft GDB format, containing the following channels:

**Table 6:** Geosoft Resistivity Depth Image GDB Data Format

Channel name	Units	Description
Xg	metres	Easting WGS84 Zone 16N
Yg	metres	Northing WGS84 Zone 16N
Dist	metres	Distance from the beginning of the line
Depth	metres	array channel, depth from the surface
Z	metres	array channel, depth
AppRes	Ohm-m	array channel, Apparent Resistivity
TR	metres	EM system height
Topo	metres	digital elevation model
Radarb	metres	Calculated EM transmitter-receiver loop terrain clearance from radar altimeter
SF	$\text{pV}/(\text{A}\cdot\text{m}^4)$	array channel, Z dB/dT
MAG	nT	TMI data
CVG	nT/m	CVG data
DOI	metres	Depth of Investigation: a measure of VTEM depth effectiveness
PLM		60Hz Power Line Monitor

- Database of the VTEM Waveform “GL210203\_Waveform.gdb” in Geosoft GDB format, containing the following channels:

**Table 7:** Geosoft database for the VTEM waveform

Channel name	Units	Description
Time	milliseconds	Sampling rate interval, 5.2083 microseconds
Tx_Current	amps	Output current of the transmitter

- Geosoft Resistivity Depth Image Products:

Sections: Apparent resistivity sections along each line in .GRD and .PDF format  
 Slices: Apparent resistivity slices at selected depths from 25m to depth of investigation, at an increment of 25m in .GRD and .PDF format  
 Voxel: 3D Voxel imaging of apparent resistivity data clipped by digital elevation and depth of investigation

- Grids in Geosoft GRD and GeoTIFF format, as follows:

GL210203\_BFz29: B-Field Z Component Channel 29 (Time Gate 0.766 ms)  
 GL210203\_SFxFF26: Fraser Filtered dB/dt X Component Channel 26 (Time Gate 0.505 ms)  
 GL210203\_SFz21: dB/dt Z Component Channel 21 (Time Gate 0.253 ms)  
 GL210203\_SFz29: dB/dt Z Component Channel 29 (Time Gate 0.766 ms)  
 GL210203\_SFz40: dB/dt Z Component Channel 35 (Time Gate 3.521 ms)  
 GL210203\_TauSF: dB/dt Z Component, Calculated Time Constant (ms)  
 GL210203\_TauBF: B-Field Z Component, Calculated Time Constant (ms)  
 GL210203\_TMI3: Total Magnetic Intensity (nT)  
 GL210203\_CVG: Calculated Vertical Derivative (nT/m)  
 GL210203\_Hginline: Measured In-Line Gradient (nT/m)  
 GL210203\_Hgcxline: Measured Cross-Line Gradient (nT/m)  
 GL210203\_TotHG: Magnetic Total Horizontal Gradient (nT/m)  
 GL210203\_TiltDrv: Magnetic Tilt derivative (radians)  
 GL210203\_DEM: Digital Elevation Model (m)  
 GL210203\_PLM: 60 Hz Power Line Monitor

A Geosoft .GRD file has a .GI metadata file associated with it, containing grid projection information. A grid cell size of 37.5 metres was used.



## 6. CONCLUSIONS AND RECOMMENDATIONS

A helicopter-borne versatile time domain electromagnetic (VTEM™plus) horizontal magnetic gradiometer geophysical survey has been completed over the Farwell Gold Copper Project near Wawa, ON, on behalf of Bold Ventures Inc.

The total area coverage is 85 km<sup>2</sup> and the total survey line coverage is 571 line kilometres over one (1) survey block. The principal sensors included a Time Domain EM system, and a horizontal magnetic gradiometer system with two caesium magnetometers. Results have been presented as stacked profiles, and contour colour images at a scale of 1:15,000. A formal interpretation has not been included in this study, however RDI resistivity-depth imaging has been performed in support of the VTEM data.

Based on the geophysical results obtained, a number of geophysical anomalies of interest have been identified across the survey area. Magnetically, the Farwell Prospect is very active, with a measured range of >9,000 nT, and featuring a prominent, large (>8x1 km), EW-elongate, lithologic-like, strongly magnetic high feature that defines the centre portion of the block and pinches towards its eastern edge. Thinner, more weakly magnetic, EW to ENE trending lineament-like horizons parallel the main feature on its north and south flanks. Low to moderate magnetic susceptibility rock occur throughout the northern half as well as the southeastern edge of the property. A strong, large (>4x4 km), intrusion-like magnetic anomaly occupies the southwestern portion of the block. An unusually straight, sharp NE-SW linear magnetic contact between moderately and weakly magnetic rocks defines the northwestern edge of the property. Numerous small (<1x1 km), intrusion-like magnetic highs also occur throughout the property.

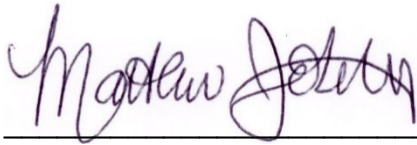
Electromagnetically, the Farwell Project hosts a mix of stratigraphic-like, moderate to long strike-length (>3-5 km), highly anomalous late-channel (>ch45) conductive horizons, found mainly in the eastern half of the block; as well as more discontinuous, discrete, short strike-length (<100-300 m), late-channel conductive anomalies in the western half of the block. These conductive features extend nearly across the central part of the block, in close association with the main magnetic high horizon and northern contact of the large intrusion-like high, described previously. A thin, middle to late-channel (>ch25-45), linear conductive EM anomaly also coincides with the sharp magnetic contact defined to the northwest. A number of small (<0.5 x 1.5 km), isolated, mid to late channel (>ch35-45) EM conductive highs are scattered the rest of the block. Most are strongly correlated with magnetic highs.

The relationship between the EM and magnetic signatures are highlighted in our TAU EM decay constant map with magnetic CVG contours (Appendix C) and the RDI resistivity-depth image sections with profiles (Appendix G). Negative EM decays, related to AIIP (airborne inductively induced polarization) are present but uncommon. Conductive anomalies feature EM dB<sub>z</sub>/dt time constants in the ~0.3-5.6 ms range, which indicates moderate to high conductivities. According to the RDI imaging results, apparent resistivities range from lows of approx. 1-30 ohm-m and reach high of approx. 3500-5500 ohm-m. Based on RDI's, the estimated depth of burial of conductive units varies from within the 75m of surface to approx. 250 m depths. Maximum depths of depths of investigation (DOI) range from ~150m in conductive regions to >700m depths in resistive rocks.

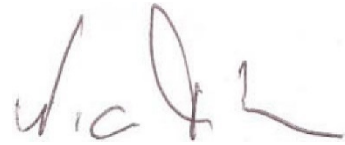
The Farwell Gold Copper Project is known to be prospective for BIF and orogenic shear-hosted gold, and also base metal VMS mineralization (Cu, Zn, Pb) related to mafic-felsic volcanic sequence ([www.boldventuresinc.com](http://www.boldventuresinc.com)). As a result, both the EM and magnetic results are likely to be of exploration interest. We recommend that EM anomaly picking be performed along with Maxwell 3D

EM plate modeling on the major anomalies of interest. AIIP (airborne inductive induced polarization) mapping may assist in defining chargeability highs related to gold mineralization or mineral alteration. CET-type magnetic lineament analysis and 3D MVI magnetic inversions will be useful for mapping structure, alteration, and lithology in 2D-3D space across the blocks. We recommend that more advanced, integrated interpretation, such as AI-assisted SOM (self-organizing maps) analysis be performed to better correlate EM and magnetic features in 3D and these results be further evaluated against the known geology for future targeting.

Respectfully submitted<sup>2</sup>.



Matthew Johnson  
**Geotech Ltd.**



Nick Venter  
**Geotech Ltd.**



Mike Finlayson  
**Geotech Ltd.**



Emily Data  
**Geotech Ltd.**



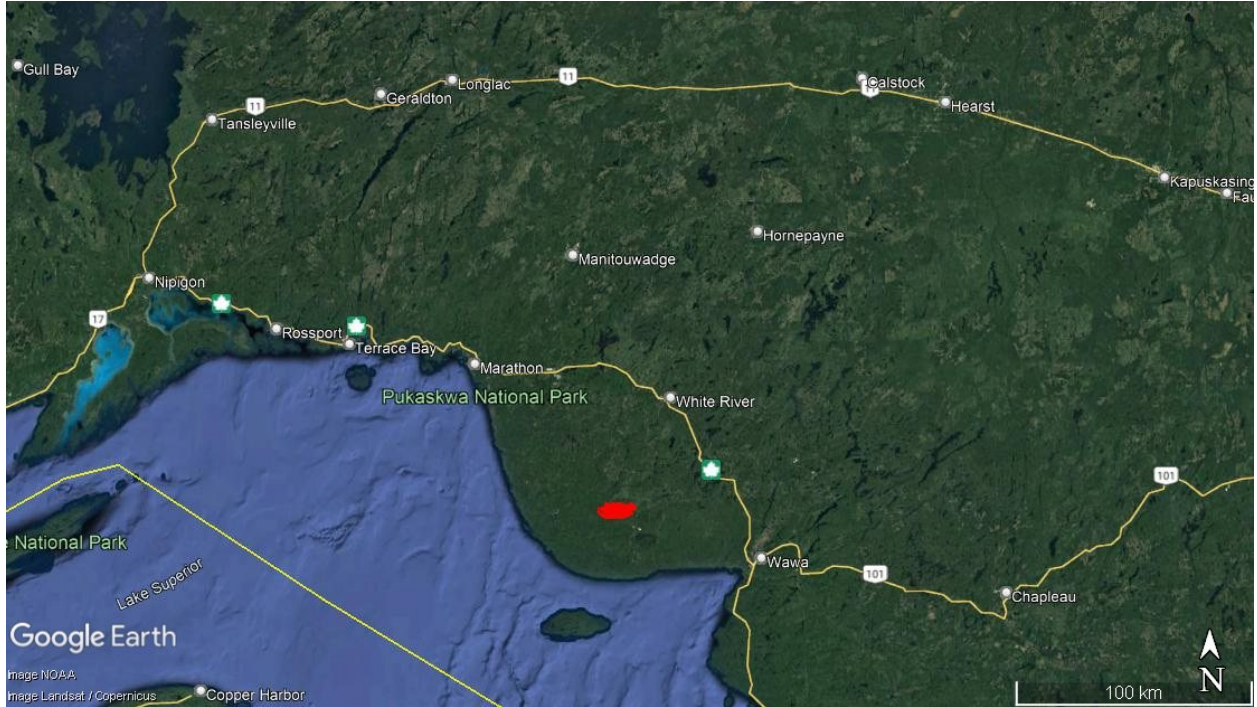
Jean M. Legault, M.Sc.A, P.Eng, P. Geo  
**Geotech Ltd.**

February 2022

<sup>2</sup>Final data processing of the EM and magnetic data was carried out by Mike Finlayson, from the offices of Geotech Ltd. in Aurora, Ontario, under the supervision of TaiChyi Shei & Jean M. Legault, Chief Geophysicist.

# APPENDIX A

## SURVEY AREA LOCATION MAP



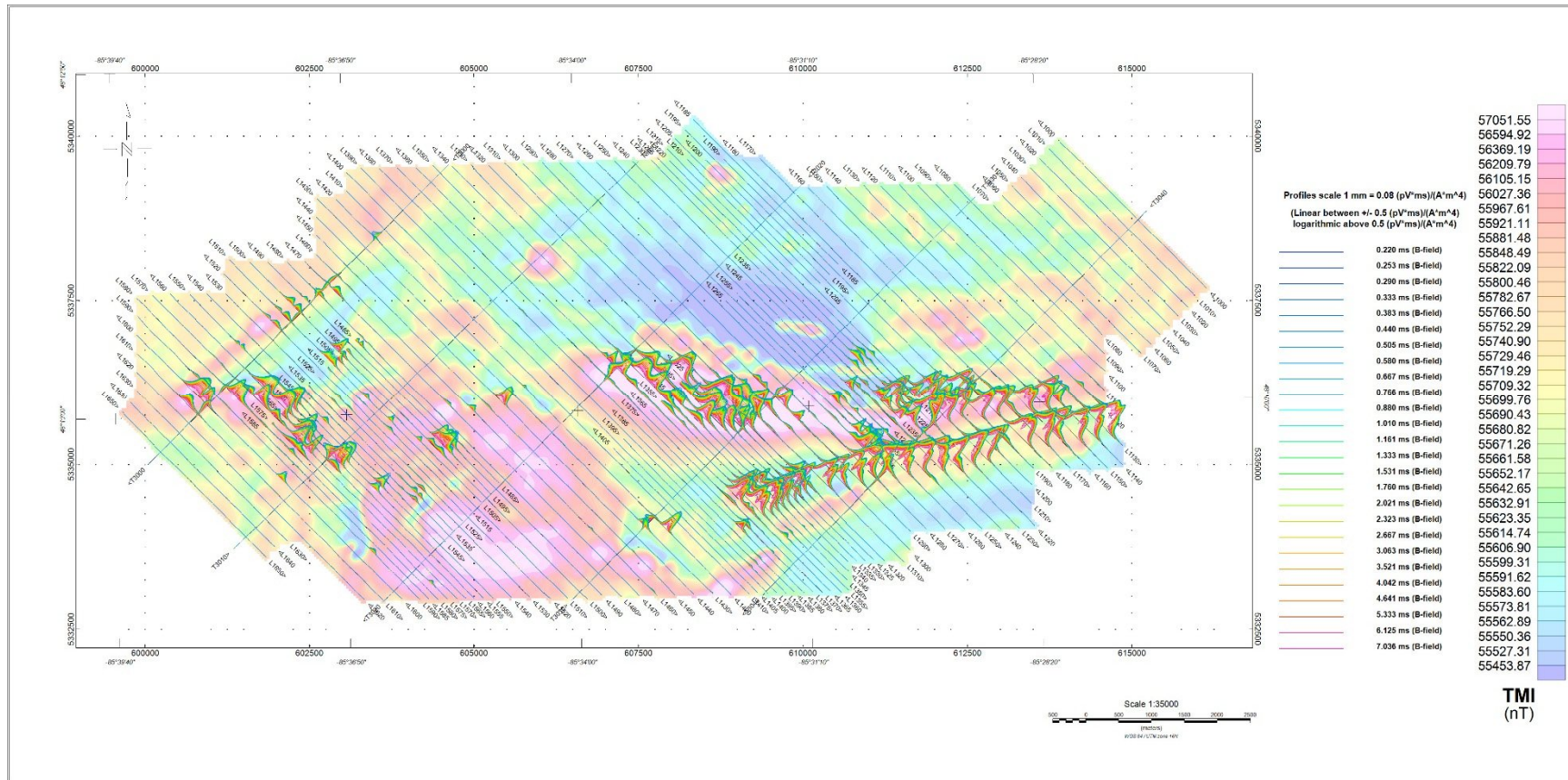
Overview of the Survey Area

## APPENDIX B

### SURVEY AREA COORDINATES (WGS84 UTM Zone 16N)

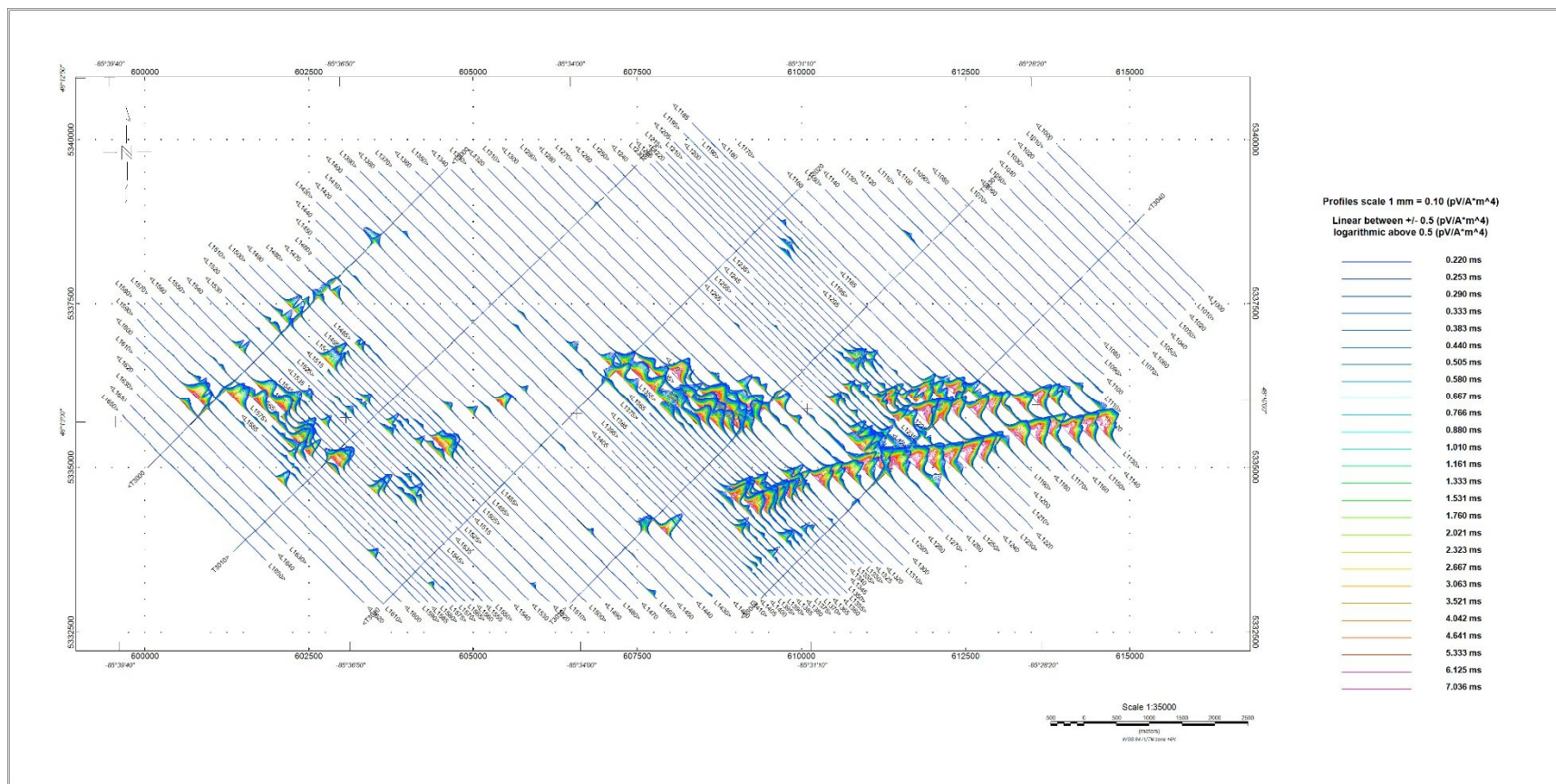
X	Y	X	Y
599600	5335819	616155	5337672
599874	5336084	615133	5336677
599856	5337307	614531	5336987
600084	5337626	614594	5335628
601243	5337626	614896	5335335
601252	5338146	614868	5335016
602594	5338183	614366	5334907
602612	5339077	613472	5334952
603068	5339150	613518	5334085
603032	5339451	613289	5334049
607704	5339625	611647	5333976
608334	5340291	611601	5333501
608954	5339643	610670	5333510
609374	5339689	610588	5333054
609858	5339205	603351	5332944
612340	5339296	602329	5333930
612733	5338849	601854	5333574
613883	5339953		

## APPENDIX C - GEOPHYSICAL MAPS<sup>1</sup>

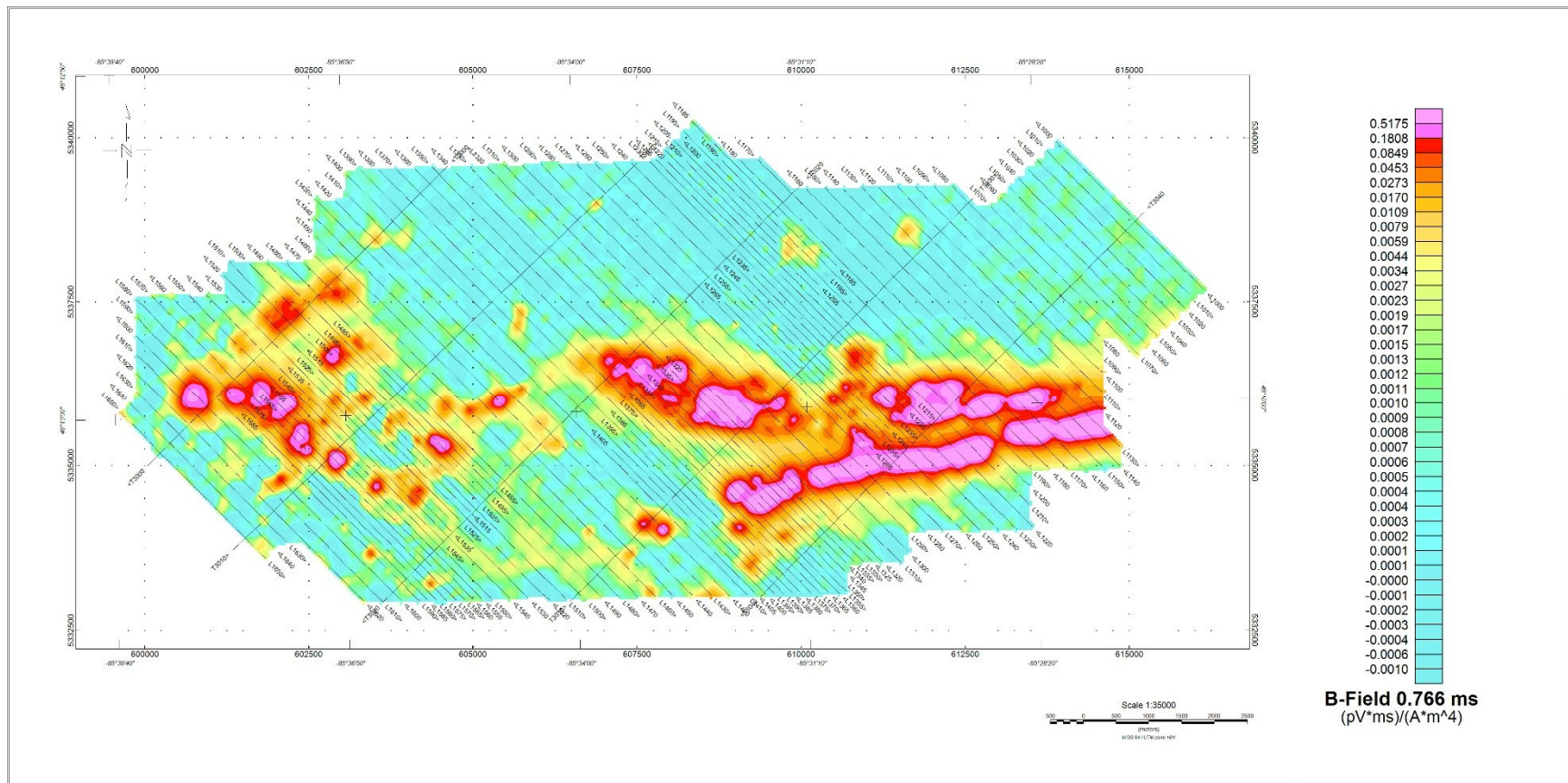


Z Component dB/dt profiles, Time Gates 0.220 – 7.036 ms

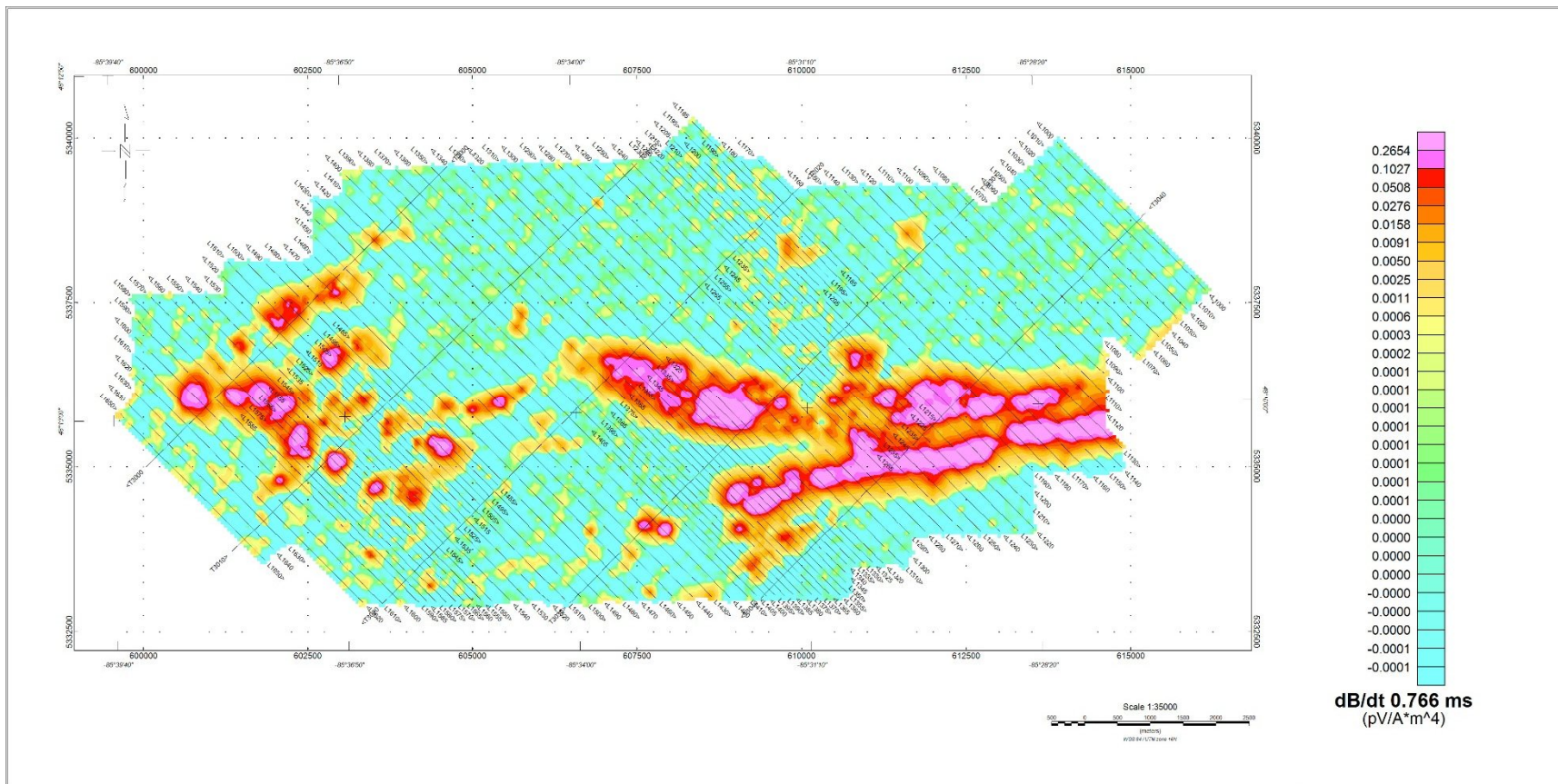
<sup>1</sup>Complete full size geophysical maps are also available in PDF format located in the final data maps folder.



Z Component B-field profiles, Time Gates 0.220 – 7.036 ms over TMI colour image

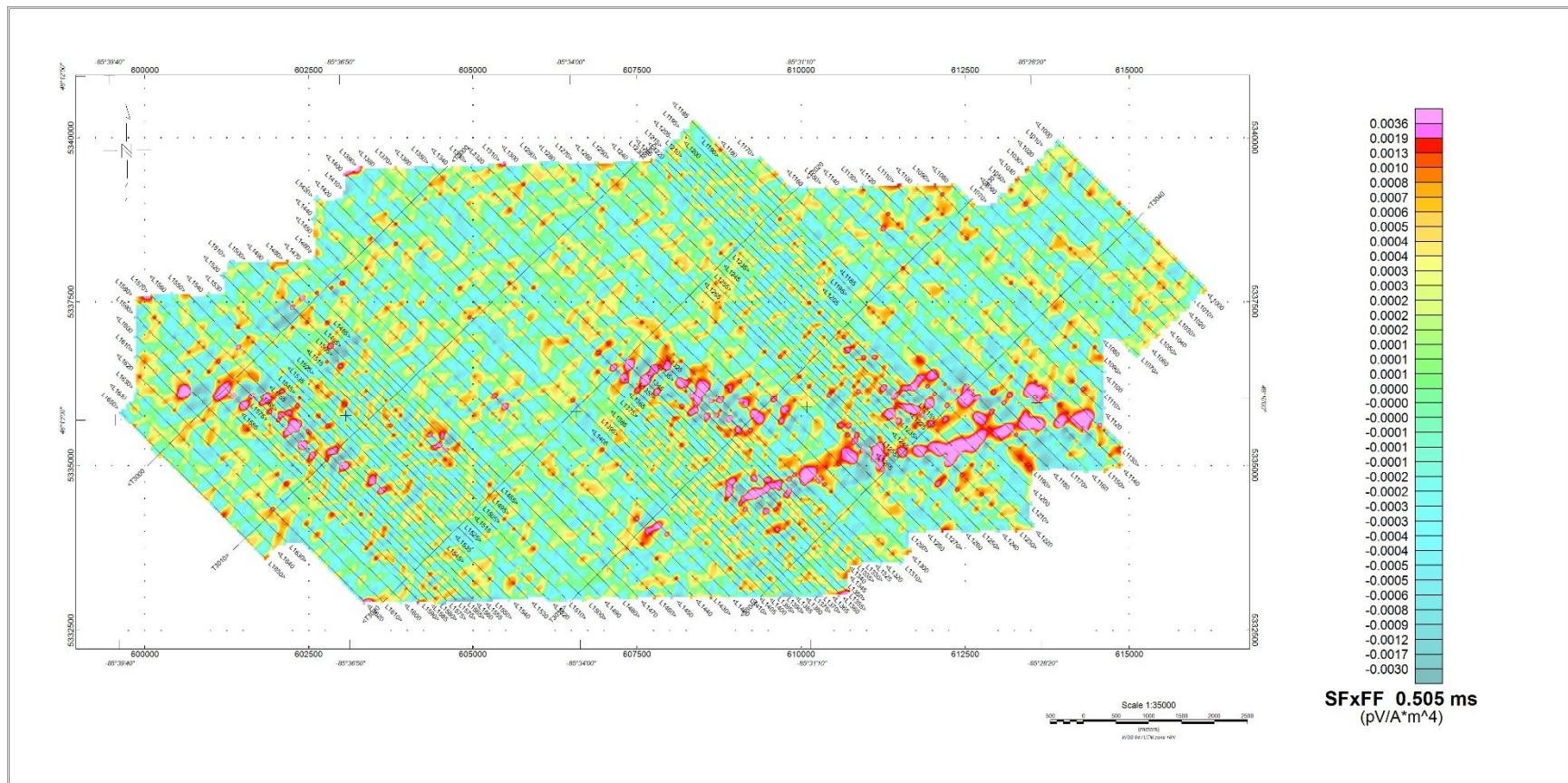


B-field Z Component Channel 29, Time Gate 0.766 ms colour image

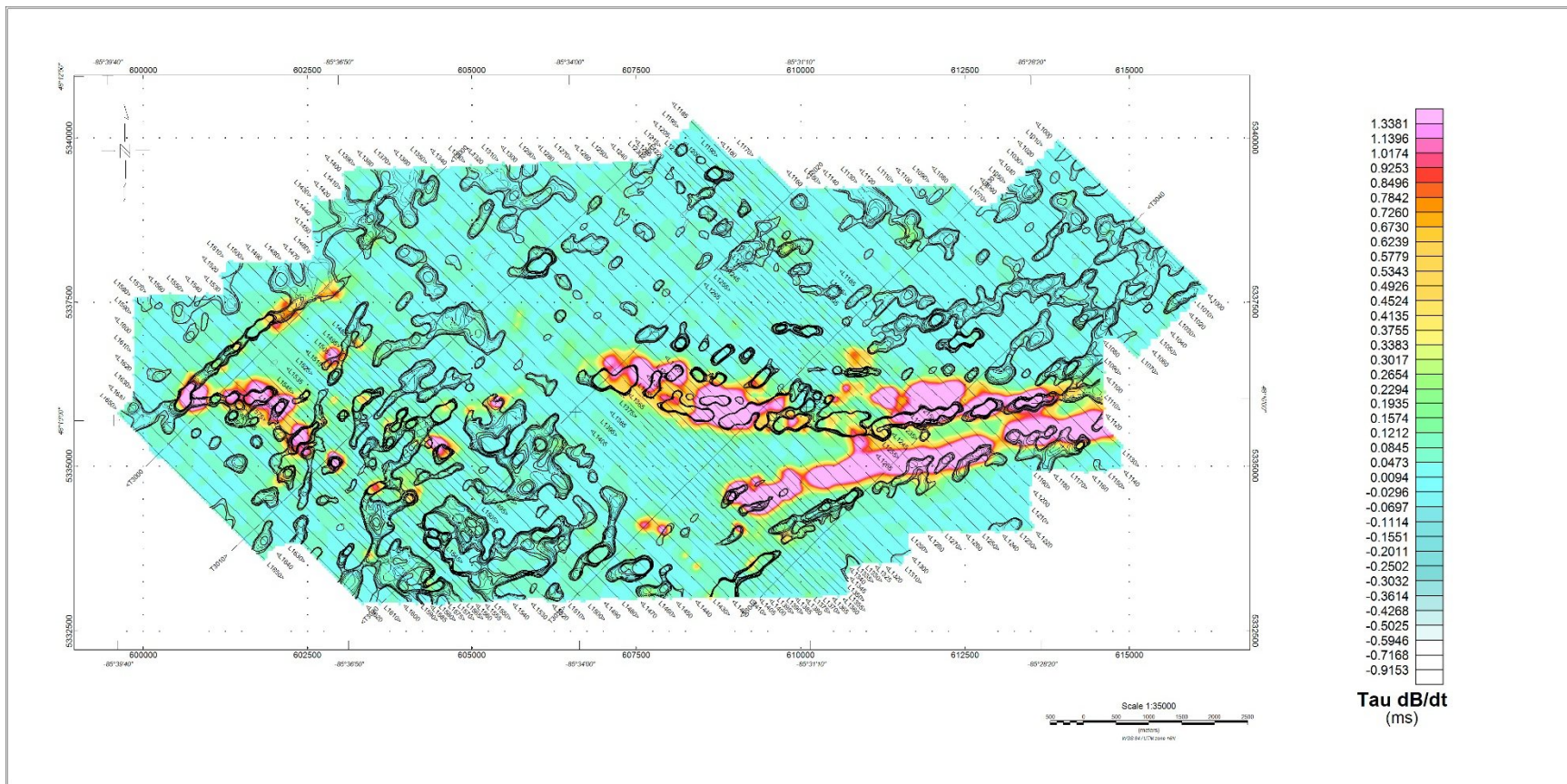


VTEM dB/dt Z Component Channel 29, Time Gate 0.766 ms colour image

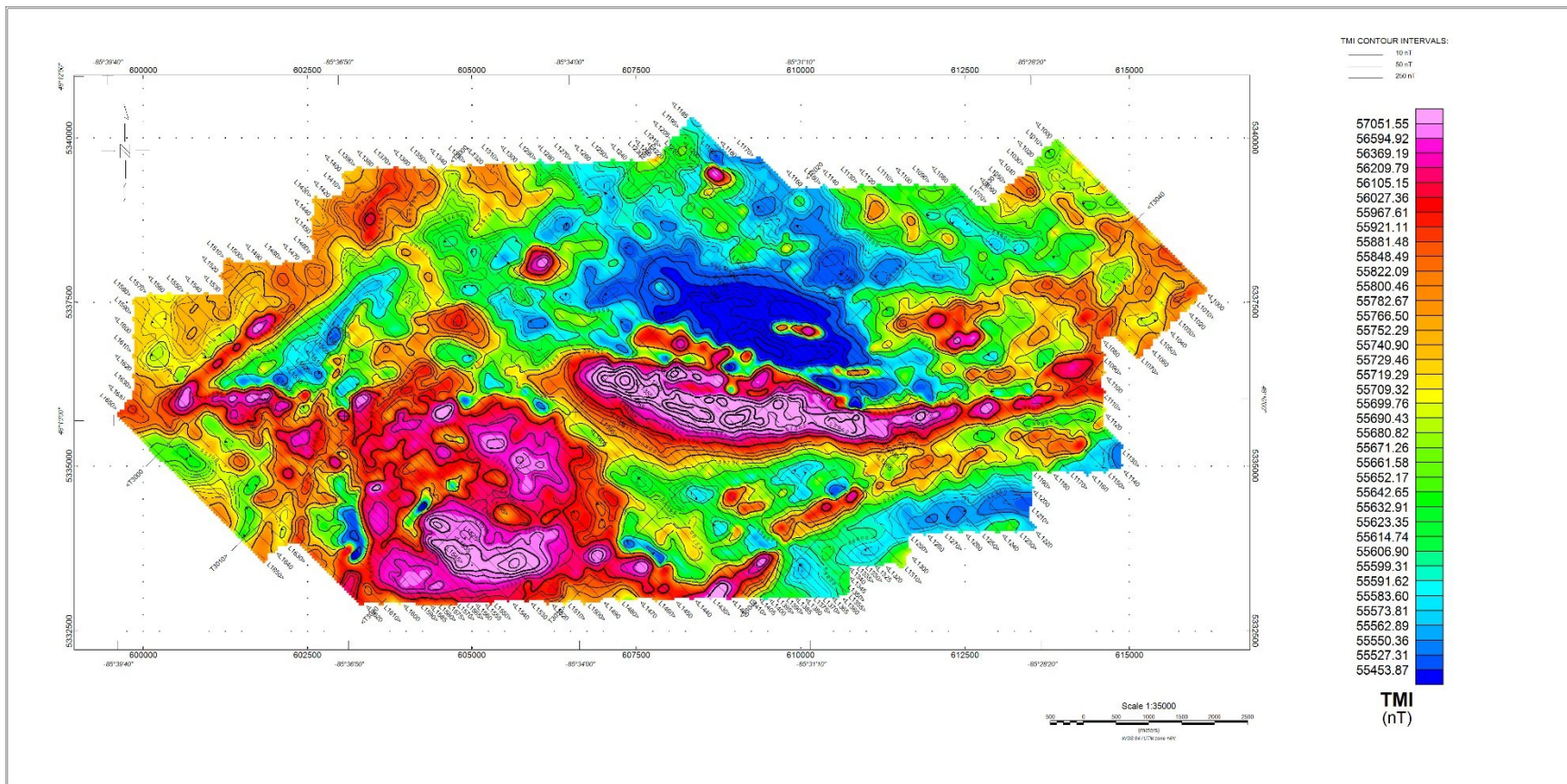




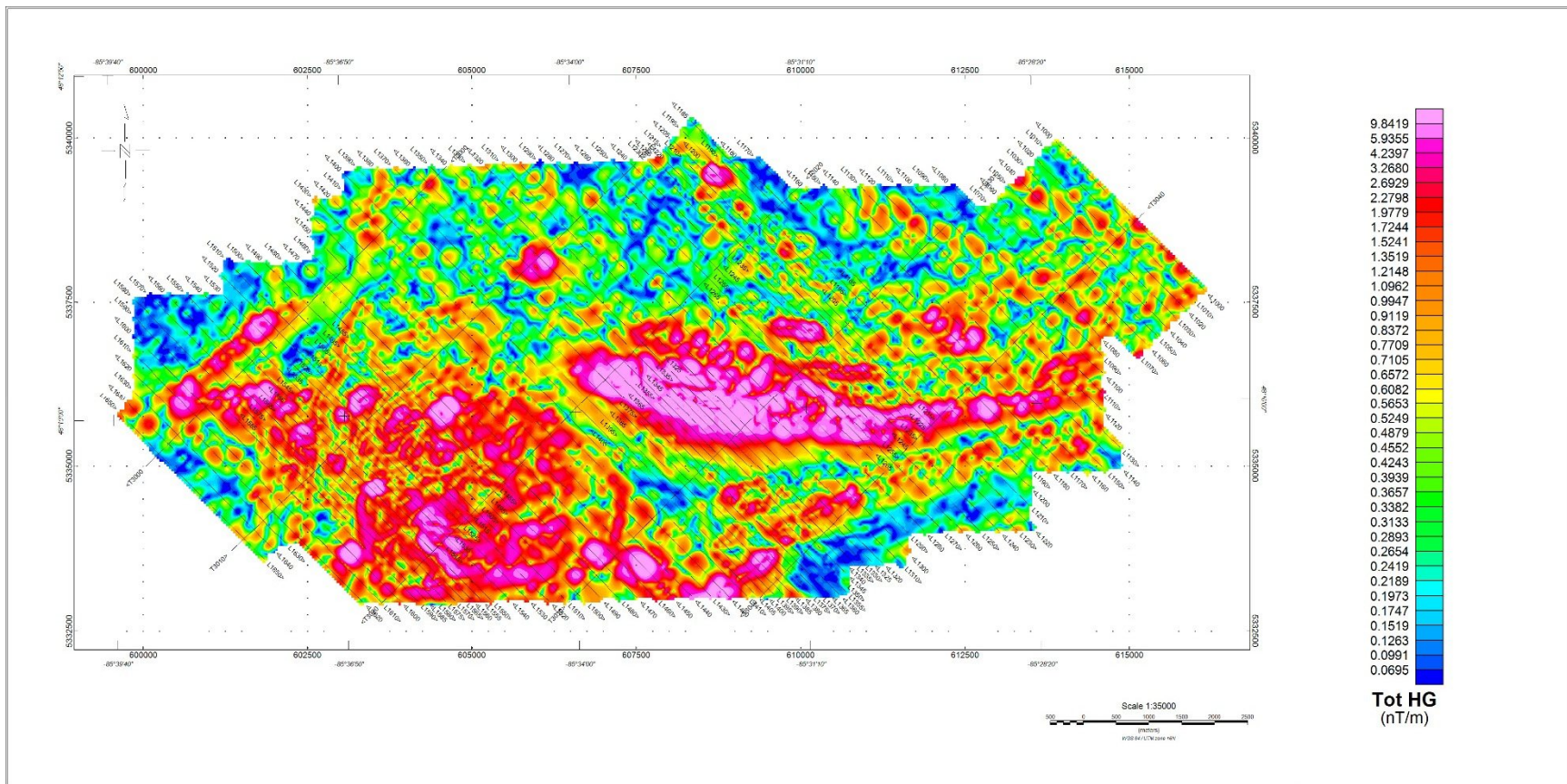
Fraser Filtered dB/dt X Component Channel 26, Time Gate 0.505 ms colour image



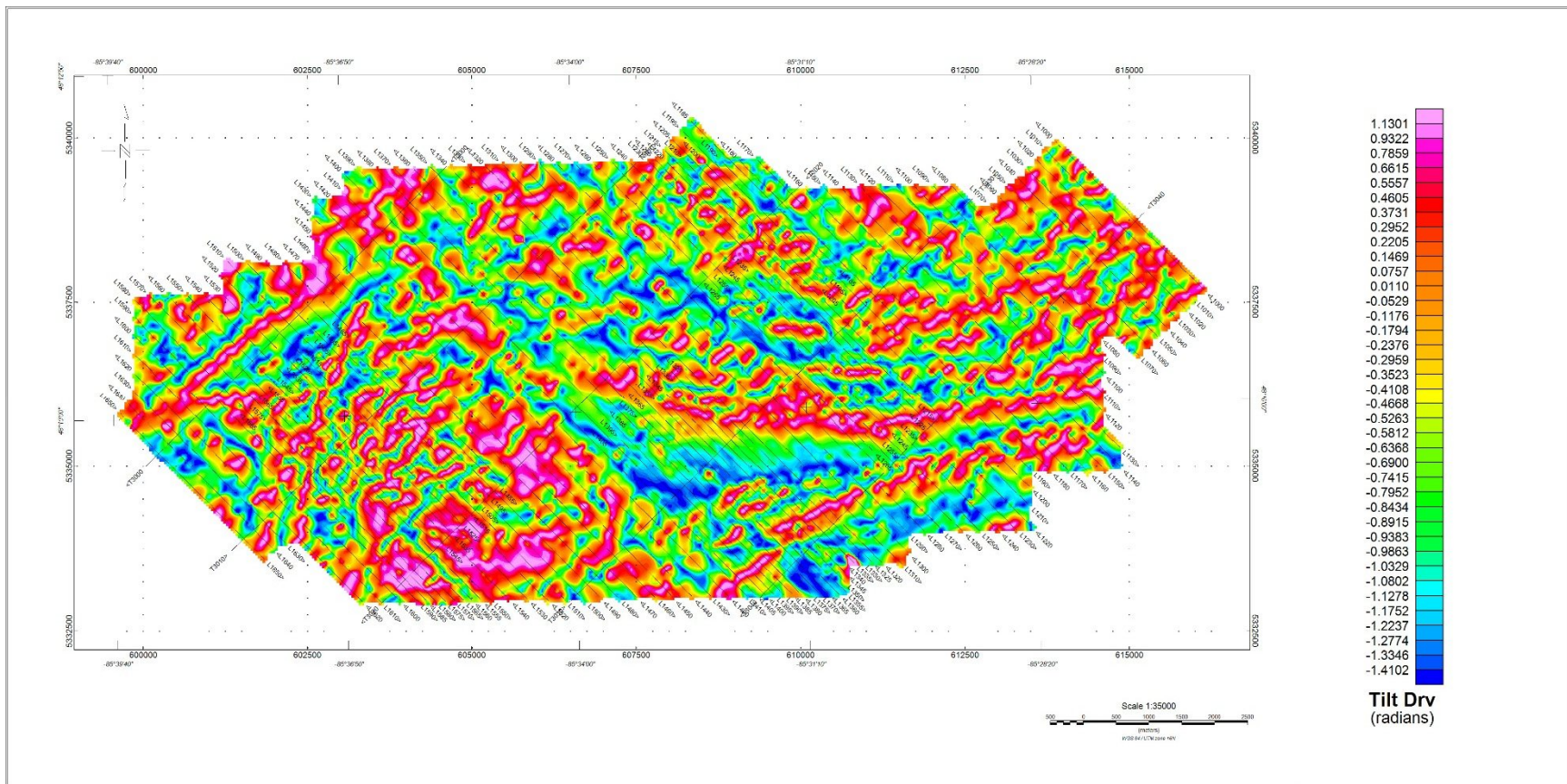
dB/dT Z-Component Calculated Time Constant (Tau) with Calculated Vertical Gradient (CVG) contours



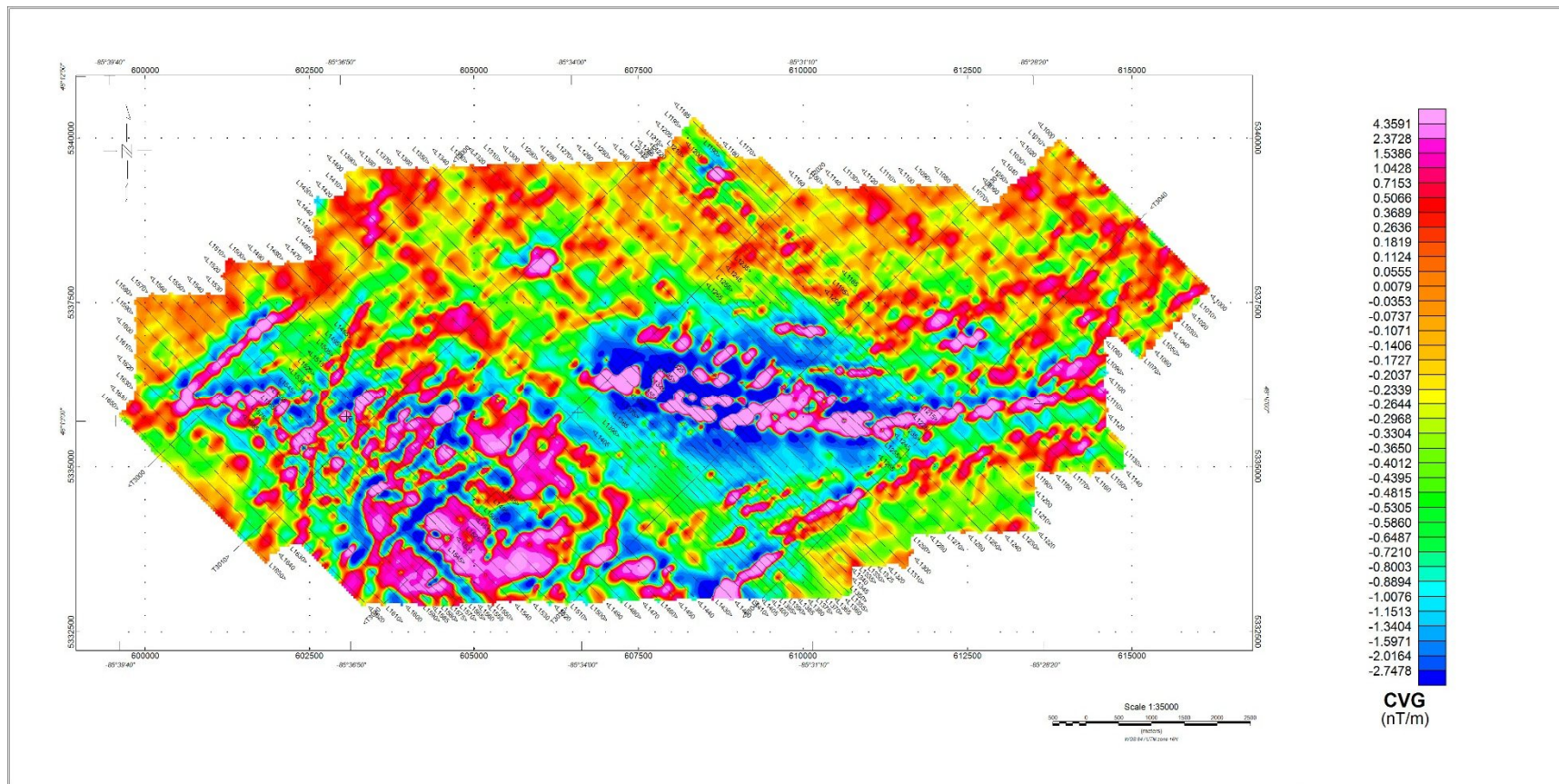
Total Magnetic Intensity (TMI) colour image and contours



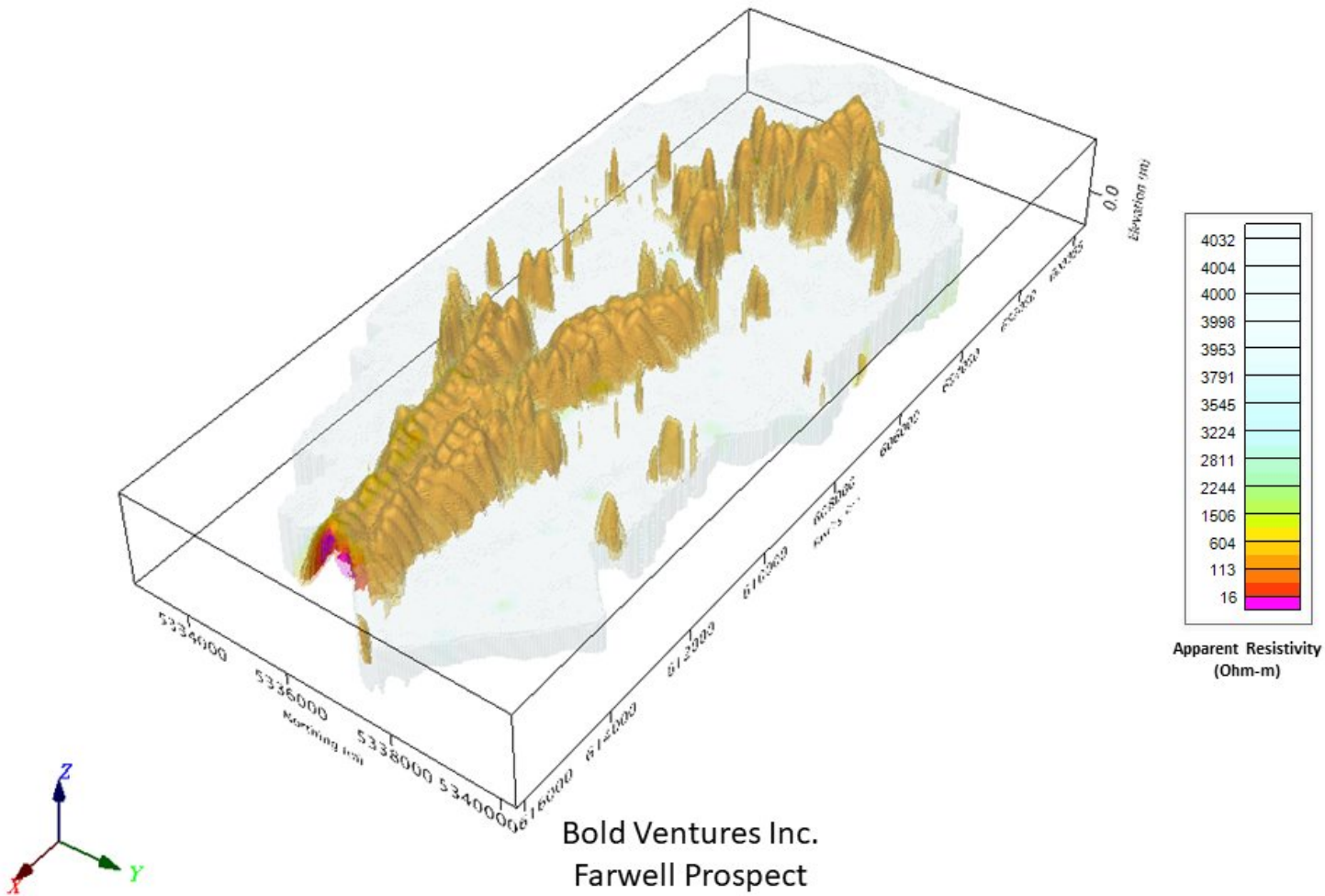
Magnetic Total Horizontal Gradient colour image



Magnetic Tilt Angle Derivative colour image



Calculated Vertical Gradient (CVG)



**Bold Ventures Inc.  
Farwell Prospect  
Near Wawa, Ontario**

3D view of Resistivity-Depth-Image (RDI), Apparent Resistivity Voxel

## APPENDIX D

### GENERALIZED MODELING RESULTS OF THE VTEM SYSTEM INTRODUCTION

The VTEM system is based on a concentric or central loop design, whereby, the receiver is positioned at the centre of a transmitter loop that produces a primary field. The wave form is a bipolar, modified square wave with a turn-on and turn-off at each end.

During turn-on and turn-off, a time varying field is produced ( $dB/dt$ ) and an electro-motive force (emf) is created as a finite impulse response. A current ring around the transmitter loop moves outward and downward as time progresses. When conductive rocks and mineralization are encountered, a secondary field is created by mutual induction and measured by the receiver at the centre of the transmitter loop.

Efficient modeling of the results can be carried out on regularly shaped geometries, thus yielding close approximations to the parameters of the measured targets. The following is a description of a series of common models made for the purpose of promoting a general understanding of the measured results.

A set of models has been produced for the Geotech VTEM™ system  $dB/dT$  Z and X components (see models D1 to D15). The Maxwell™ modeling program (EMIT Technology Pty. Ltd. Midland, WA, AU) used to generate the following responses assumes a resistive half-space. The reader is encouraged to review these models, so as to get a general understanding of the responses as they apply to survey results. While these models do not begin to cover all possibilities, they give a general perspective on the simple and most commonly encountered anomalies.

As the plate dips and departs from the vertical position, the peaks become asymmetrical.

As the dip increases, the aspect ratio (Min/Max) decreases, and this aspect ratio can be used as an empirical guide to dip angles from near  $90^\circ$  to about  $30^\circ$ . The method is not sensitive enough where dips are less than about  $30^\circ$ .



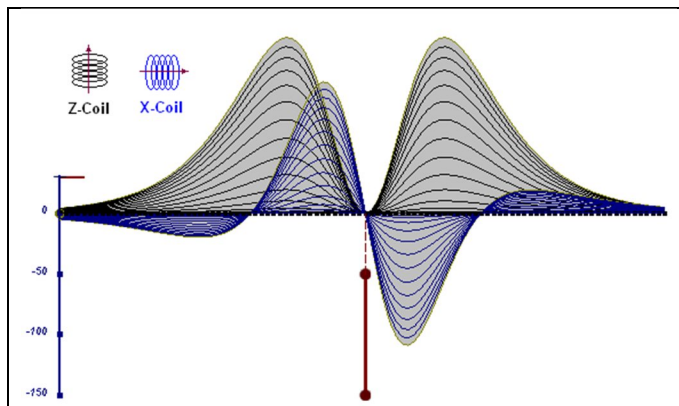


**Figure D-1:** vertical thin plate

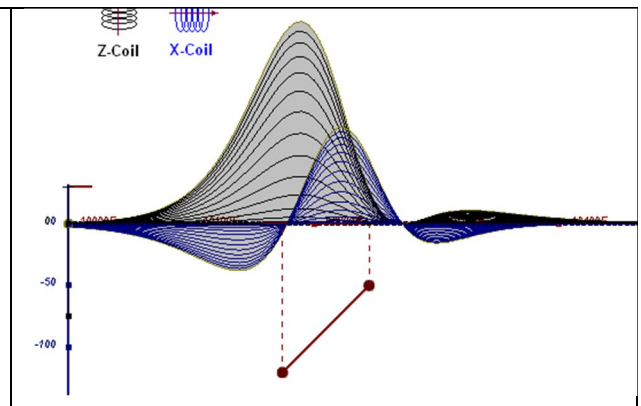


**Figure D-2:** inclined thin plate

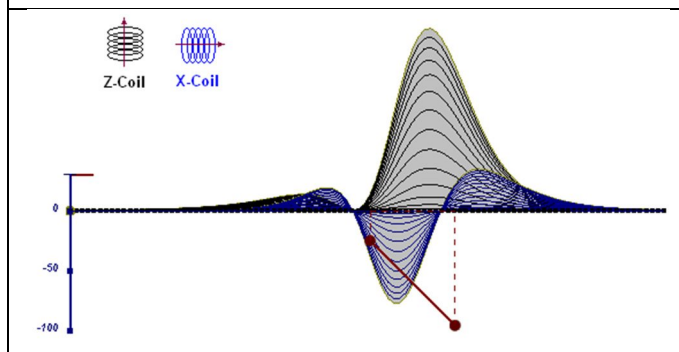


**Figure D-3:** inclined thin plate

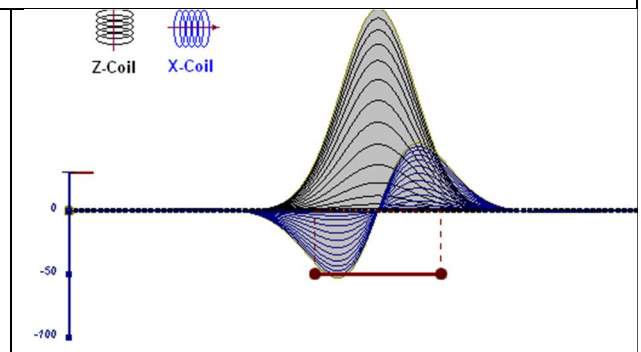


**Figure D-4:** horizontal thin plate

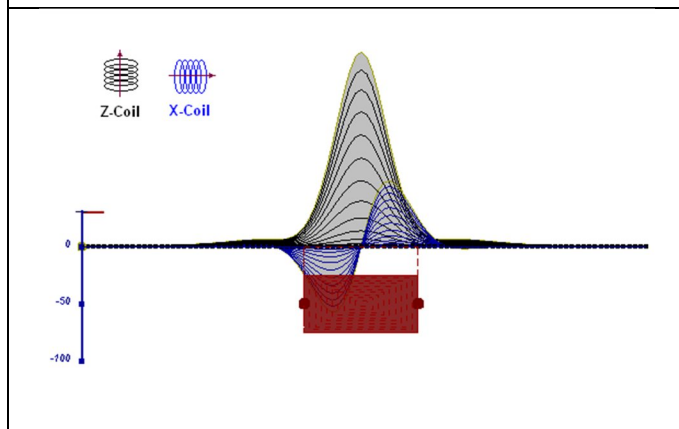


**Figure D-5:** horizontal thick plate (linear scale of the response)

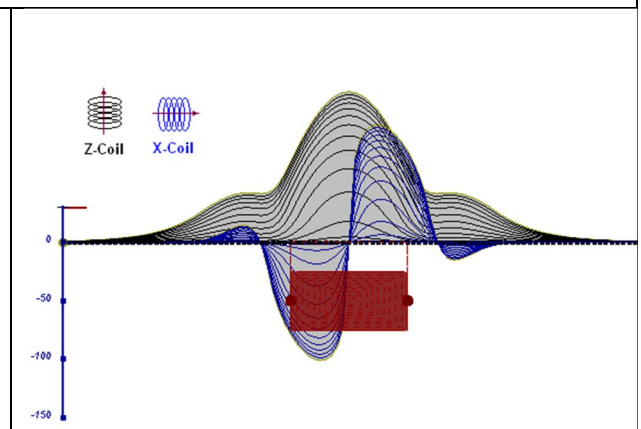


**Figure D-6:** horizontal thick plate (log scale of the response)

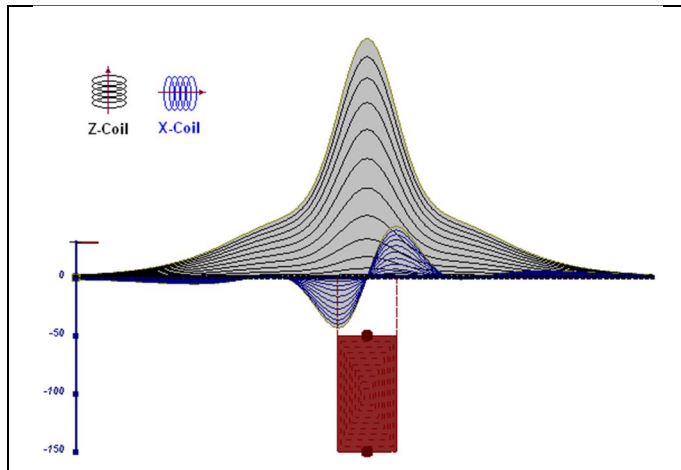


**Figure D-7:** vertical thick plate (linear scale of the response). 50 m depth

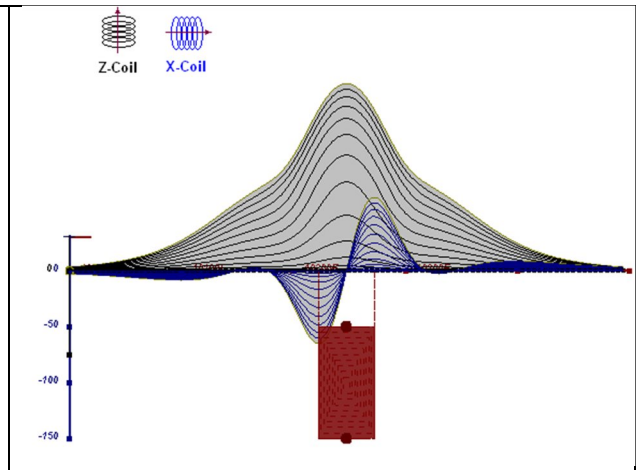


**Figure D-8:** vertical thick plate (log scale of the response). 50 m depth

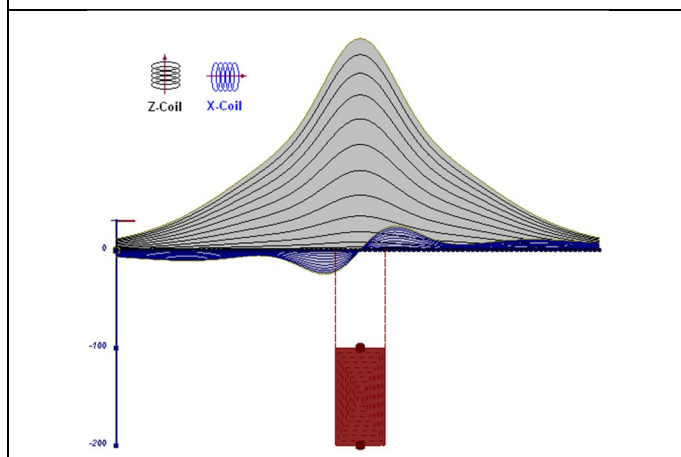


**Figure D-9:** vertical thick plate (linear scale of the response). 100 m depth

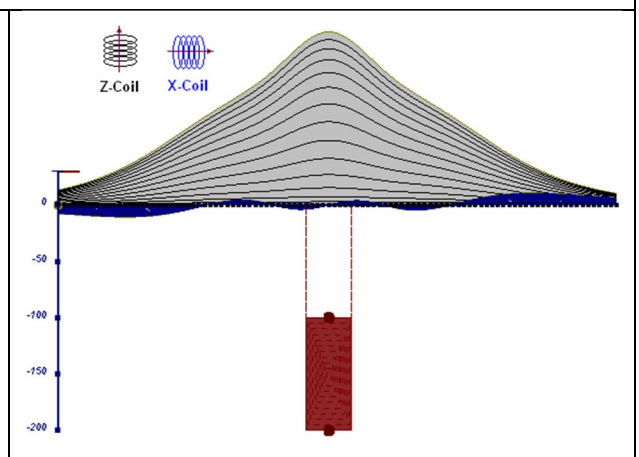


**Figure D-10:** vertical thick plate (linear scale of the response). Depth / horizontal thickness=2.5

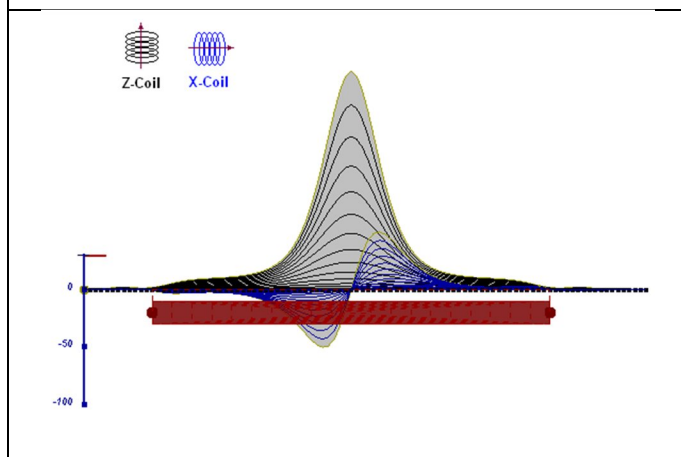


**Figure D-11:** horizontal thick plate (linear scale of the response)

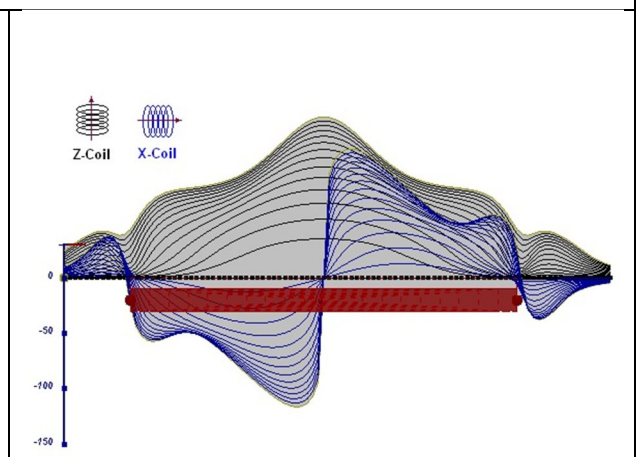


**Figure D-12:** horizontal thick plate (log scale of the response)

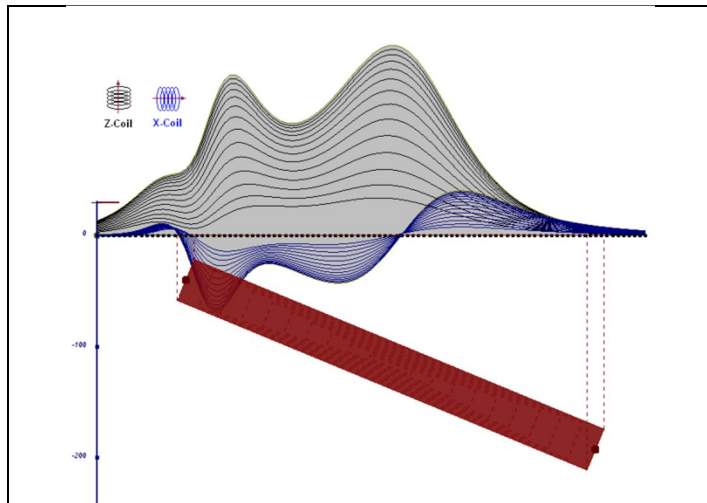


**Figure D-13:** inclined long thick plate

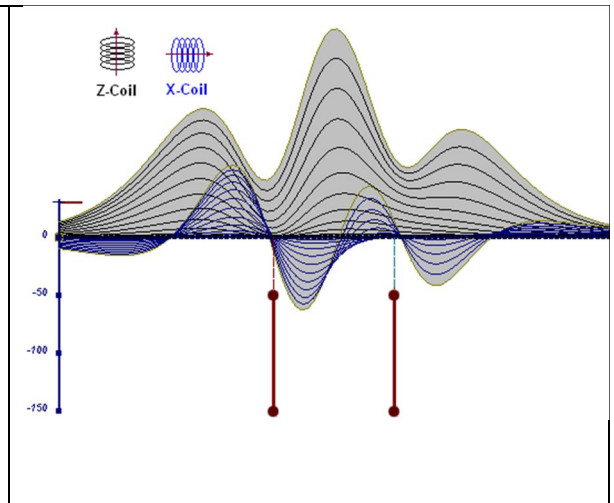


**Figure D-14:** two vertical thin plates

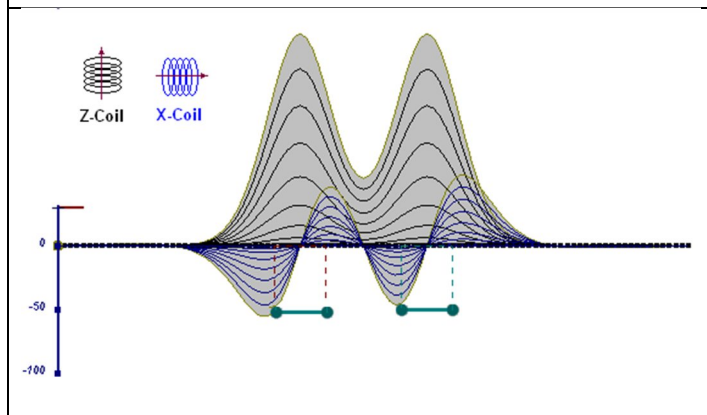


**Figure D-15:** two horizontal thin plates

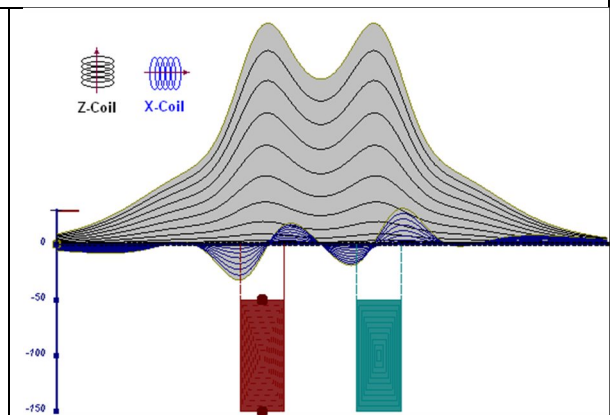


**Figure D-16:** two vertical thick plates

The same type of target but with different thickness, for example, creates different form of the response:

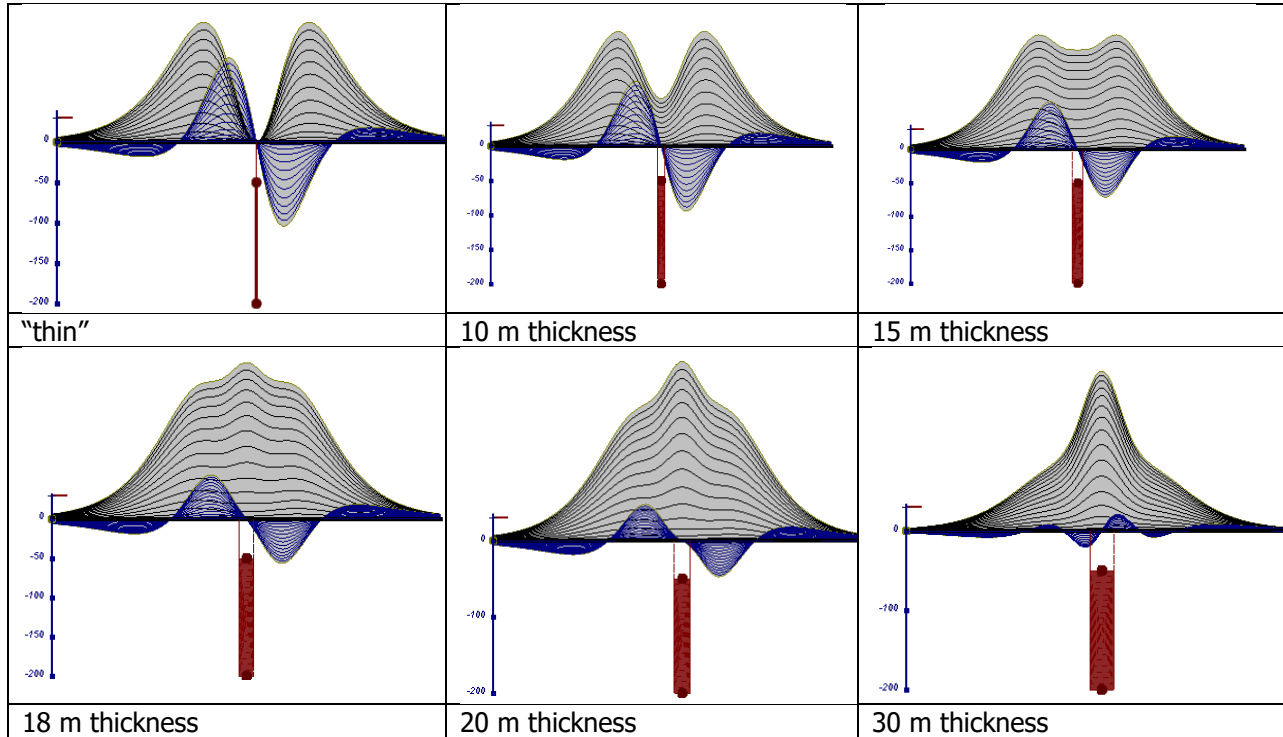


**Figure E-17:** Conductive vertical plate, depth 50 m, strike length 200 m, depth extends 150 m.

**Geotech Ltd.**

September 2010

## APPENDIX E

### EM TIME CONSTANT (TAU) ANALYSIS

Estimation of time constant parameter<sup>1</sup> in transient electromagnetic method is one of the steps toward the extraction of the information about conductances beneath the surface from TEM measurements.

The most reliable method to discriminate or rank conductors from overburden, background or one and other is by calculating the EM field decay time constant (TAU parameter), which directly depends on conductance despite their depth and accordingly amplitude of the response.

#### Theory

As established in electromagnetic theory, the magnitude of the electro-motive force (emf) induced is proportional to the time rate of change of primary magnetic field at the conductor. This emf causes eddy currents to flow in the conductor with a characteristic transient decay, whose Time Constant (Tau) is a function of the conductance of the survey target or conductivity and geometry (including dimensions) of the target. The decaying currents generate a proportional secondary magnetic field, the time rate of change of which is measured by the receiver coil as induced voltage during the Off time.

The receiver coil output voltage ( $e_0$ ) is proportional to the time rate of change of the secondary magnetic field and has the form,

$$e_0 \propto (1 / \tau) e^{-(t / \tau)}$$

Where,

$\tau = L/R$  is the characteristic time constant of the target (TAU)

R = resistance

L = inductance

From the expression, conductive targets that have small value of resistance and hence large value of  $\tau$  yield signals with small initial amplitude that decays relatively slowly with progress of time. Conversely, signals from poorly conducting targets that have large resistance value and small  $\tau$ , have high initial amplitude but decay rapidly with time<sup>1</sup>(Fig. E1).

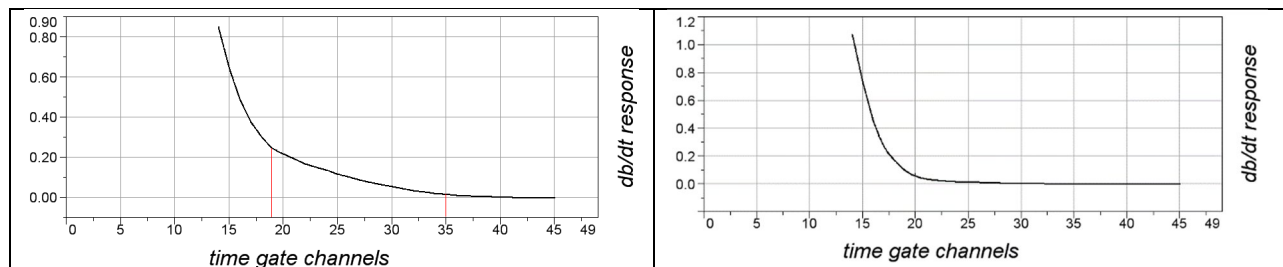


**Figure E-1:**Left – presence of good conductor, right – poor conductor.

<sup>1</sup>McNeill, JD, 1980, "Applications of Transient Electromagnetic Techniques", Technical Note TN-7 page 5, Geonics Limited, Mississauga, Ontario.

## EM Time Constant (Tau) Calculation

The EM Time-Constant (TAU) is a general measure of the speed of decay of the electromagnetic response and indicates the presence of eddy currents in conductive sources as well as reflecting the “conductance quality” of a source. Although TAU can be calculated using either the measured dB/dt decay or the calculated B-field decay, dB/dt is commonly preferred due to better stability (S/N) relating to signal noise. Generally, TAU calculated on base of early time response reflects both near surface overburden and poor conductors whereas, in the late ranges of time, deep and more conductive sources, respectively. For example, early time TAU distribution in an area that indicates conductive overburden is shown in Figure 2.

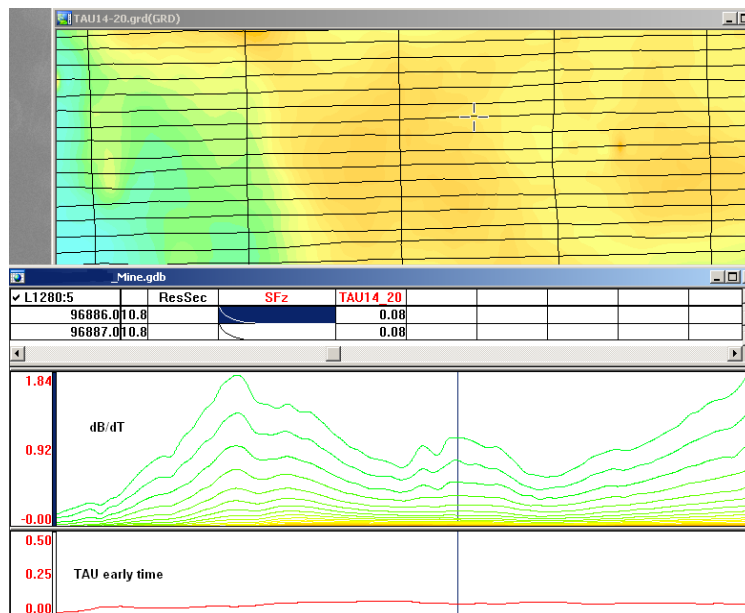


**Figure E-2:** Map of early time TAU. Area with overburden conductive layer and local sources.

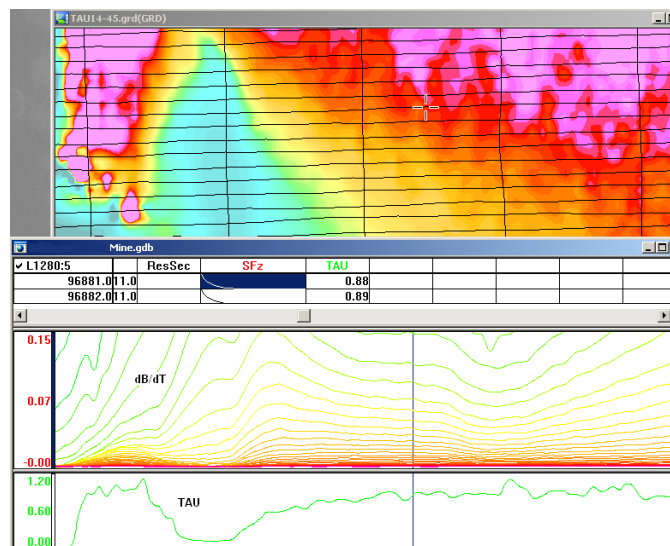


**Figure E-3:** Map of full-time range TAU with EM anomaly due to deep highly conductive target.

There are many advantages of TAU maps:

- TAU depends only on one parameter (conductance) in contrast to response magnitude.
- TAU is integral parameter, which covers time range, and all conductive zones and targets are displayed independently of their depth and conductivity on a single map.
- Very good differential resolution in complex conductive places with many sources with different conductivity.
- Signs of the presence of good conductive targets are amplified and emphasized independently of their depth and level of response accordingly.

In the example shown in Figure 4 and 5, three local targets are defined, each of them with a different depth of burial, as indicated on the resistivity depth image (RDI). All are very good conductors, but the deeper target (number 2) has a relatively weak dB/dt signal yet also features the strongest total TAU (Figure 4). This example highlights the benefit of TAU analysis in terms of an additional target discrimination tool.

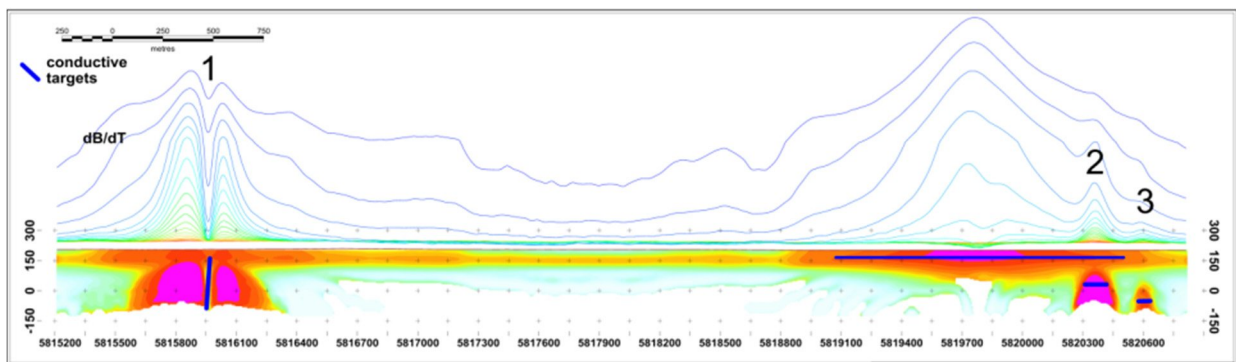


**Figure E-4:** dB/dt profile and RDI with different depths of targets.

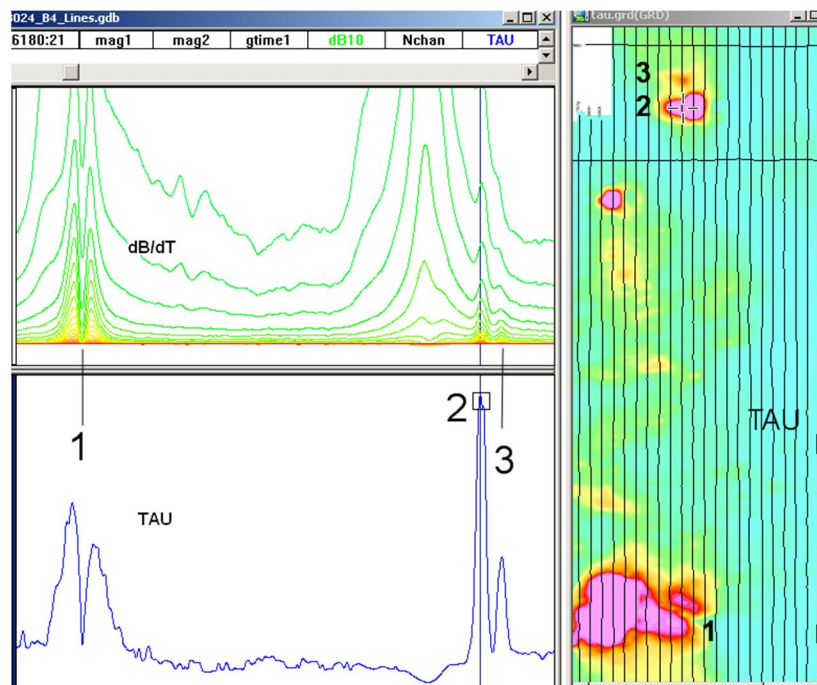


**Figure E-5:** Map of total TAU and dB/dt profile.

The EM Time Constants for dB/dt and B-field were calculated using the “sliding Tau” in-house program developed at Geotech. The principle of the calculation is based on using of time window (4 time channels) which is sliding along the curve decay and looking for latest time channels which have a response above the level of noise and decay. The EM decays are obtained from all available decay channels, starting at the latest channel. Time constants are taken from a least square fit of a straight-line (log/linear space) over the last 4 gates above a pre-set signal threshold level (Figure E6). Threshold settings are pointed in the “label” property of TAU database channels. The sliding Tau method determines that, as the amplitudes increase, the time-constant is taken at progressively later times in the EM decay. Conversely, as the amplitudes decrease, Tau is taken at progressively earlier times in the decay. If the maximum signal amplitude falls below the threshold or becomes negative for any of the 4 time gates, then Tau is not calculated and is assigned a value of “dummy” by default.

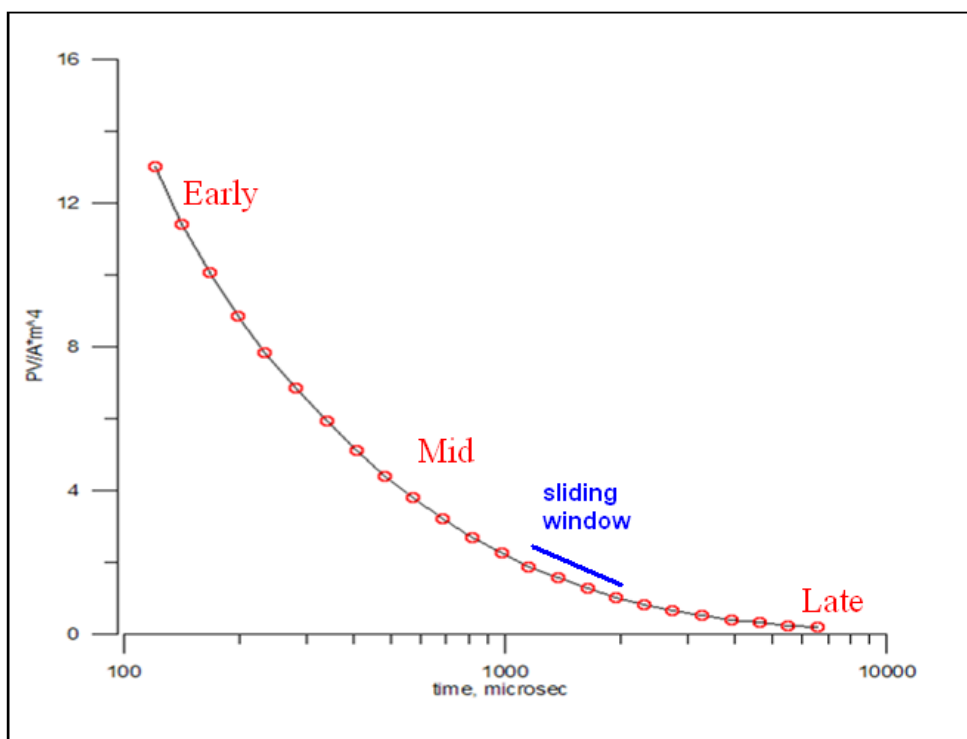


**Figure E-6:** Typical dB/dt decays of Vtem data

**Geotech Ltd.**

December 2021



## APPENDIX F

### TEM RESISTIVITY DEPTH IMAGING (RDI)

Resistivity depth imaging (RDI) is a technique used to rapidly convert EM profile decay data into an equivalent resistivity versus depth cross-section, by deconvolving the measured TEM data. The used RDI algorithm of Resistivity-Depth transformation is based on the scheme of the apparent resistivity transform of Meju (1998)<sup>1</sup> and TEM response from a conductive half-space. The program is developed by Geotech Ltd. and is depth-calibrated based on forward plate modeling for VTEM system configuration (Fig. 1-10).

RDIs provide reasonable indications of conductor relative depth and vertical extent, as well as accurate 1D layered-earth apparent conductivity/resistivity structure across VTEM flight lines. Approximate depth of investigation of a TEM system, image of secondary field distribution in half-space, effective resistivity, initial geometry and position of conductive targets is the information obtained on the basis of the RDIs.

Maxwell plate EM forward modeling with RDI sections from the synthetic responses (VTEM system) are presented below.

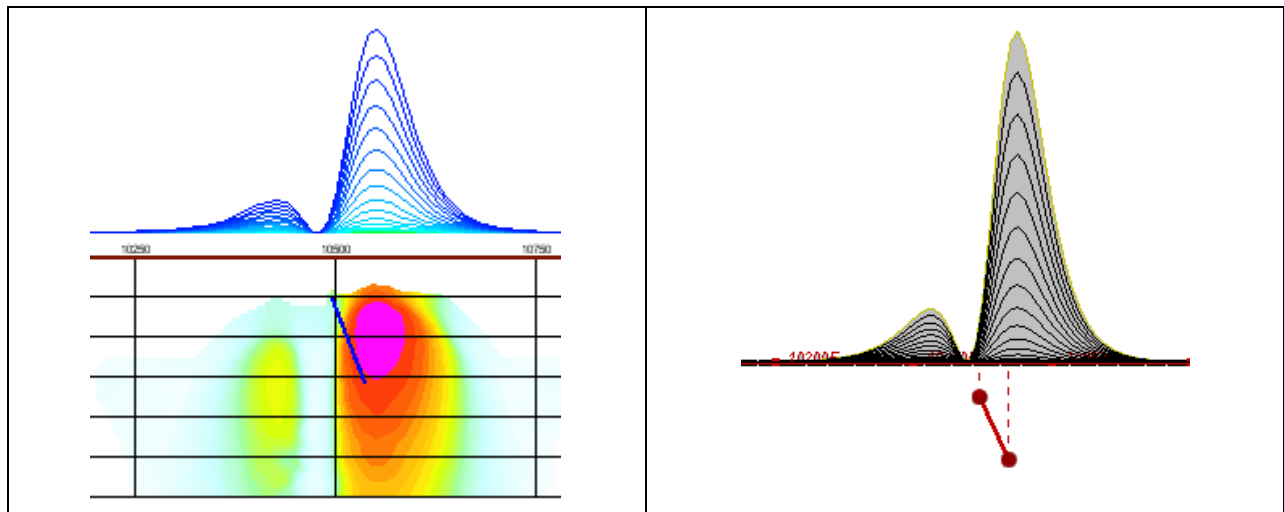


**Figure F-1:** Maxwell plate model and RDI from the calculated response for a conductive "thin" plate (depth 50 m, dip 65 degrees, depth extend 100 m).

<sup>1</sup>Maxwell A.Meju, 1998, Short Note: A simple method of transient electromagnetic data analysis, *Geophysics*, **63**, 405–410.

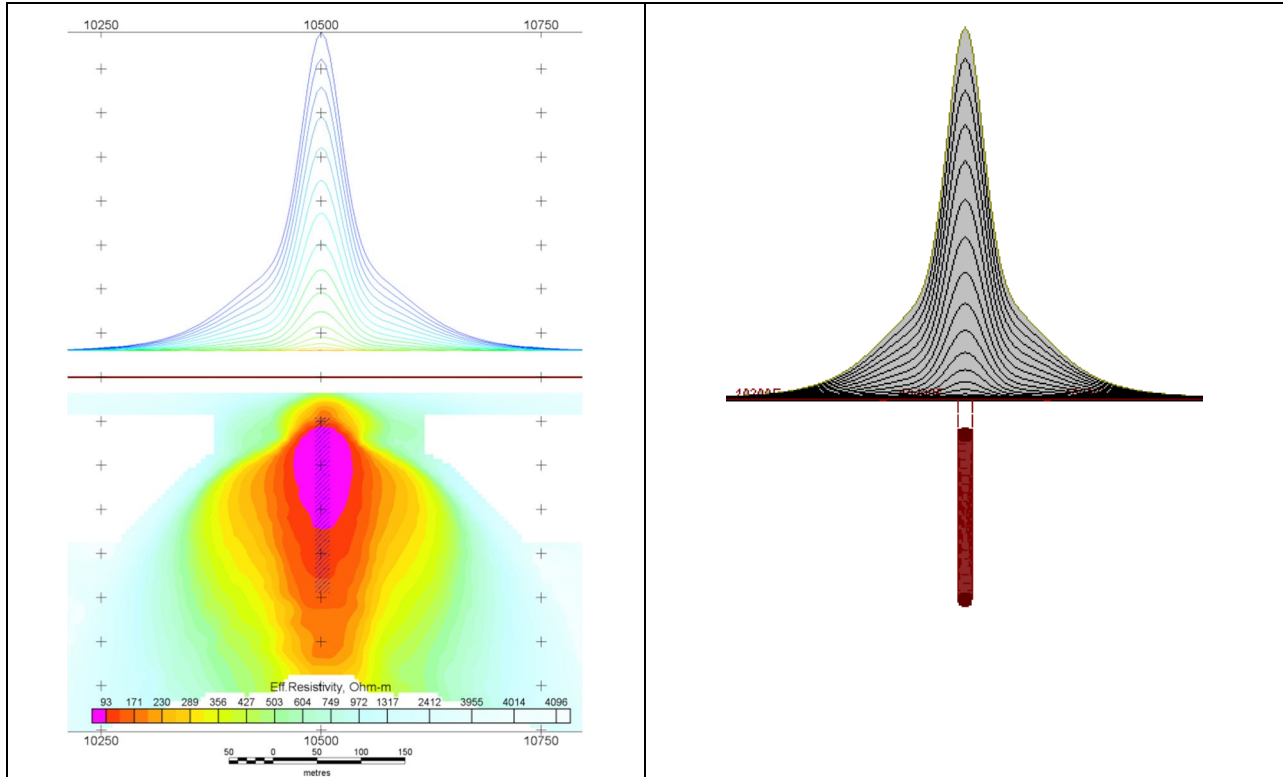


**Figure F-2:** Maxwell plate model and RDI from the calculated response for "thick" plate 18 m thickness, depth 50 m, depth extend 200 m).

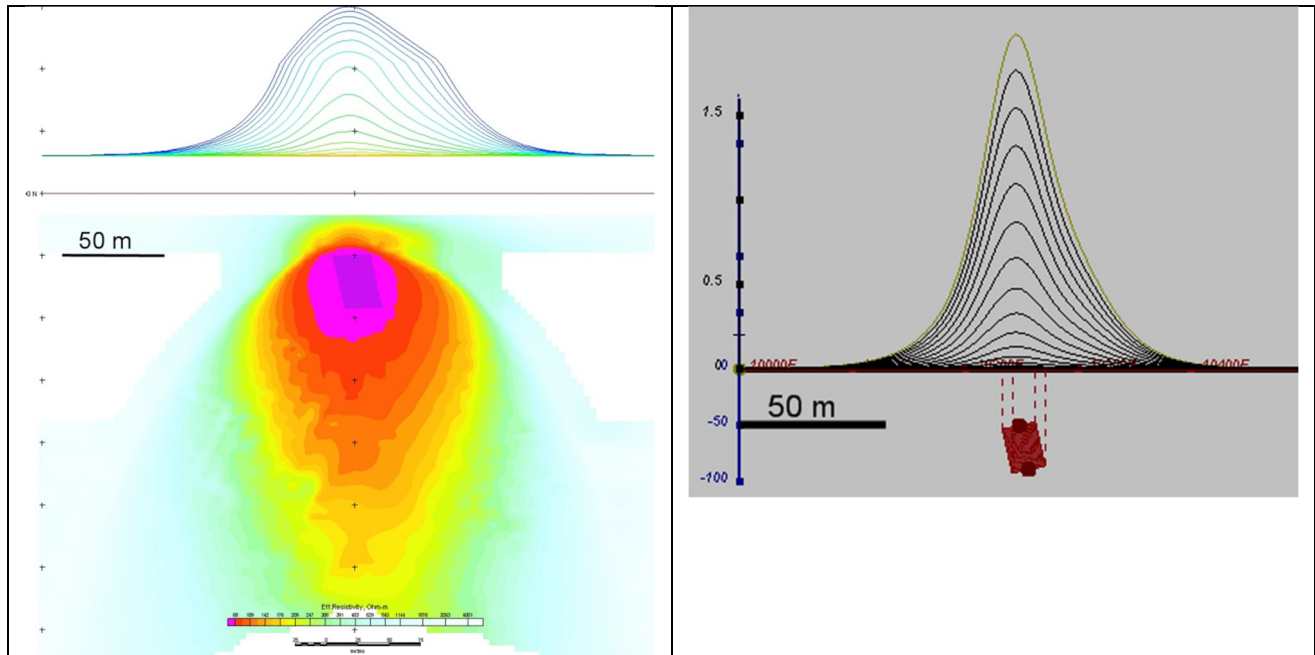


**Figure F-3:** Maxwell plate model and RDI from the calculated response for bulk ("thick") 100 m length, 40 m depth extend, 30 m thickness.

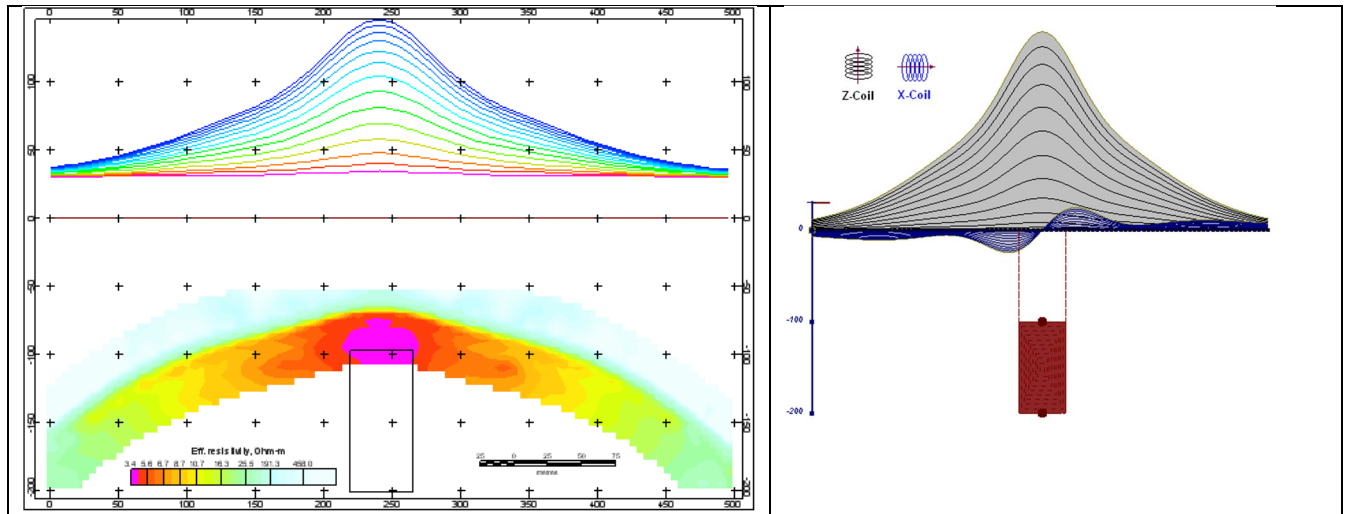


**Figure F-4:** Maxwell plate model and RDI from the calculated response for “thick” vertical target (depth 100 m, depth extend 100 m). 19-44 chan.

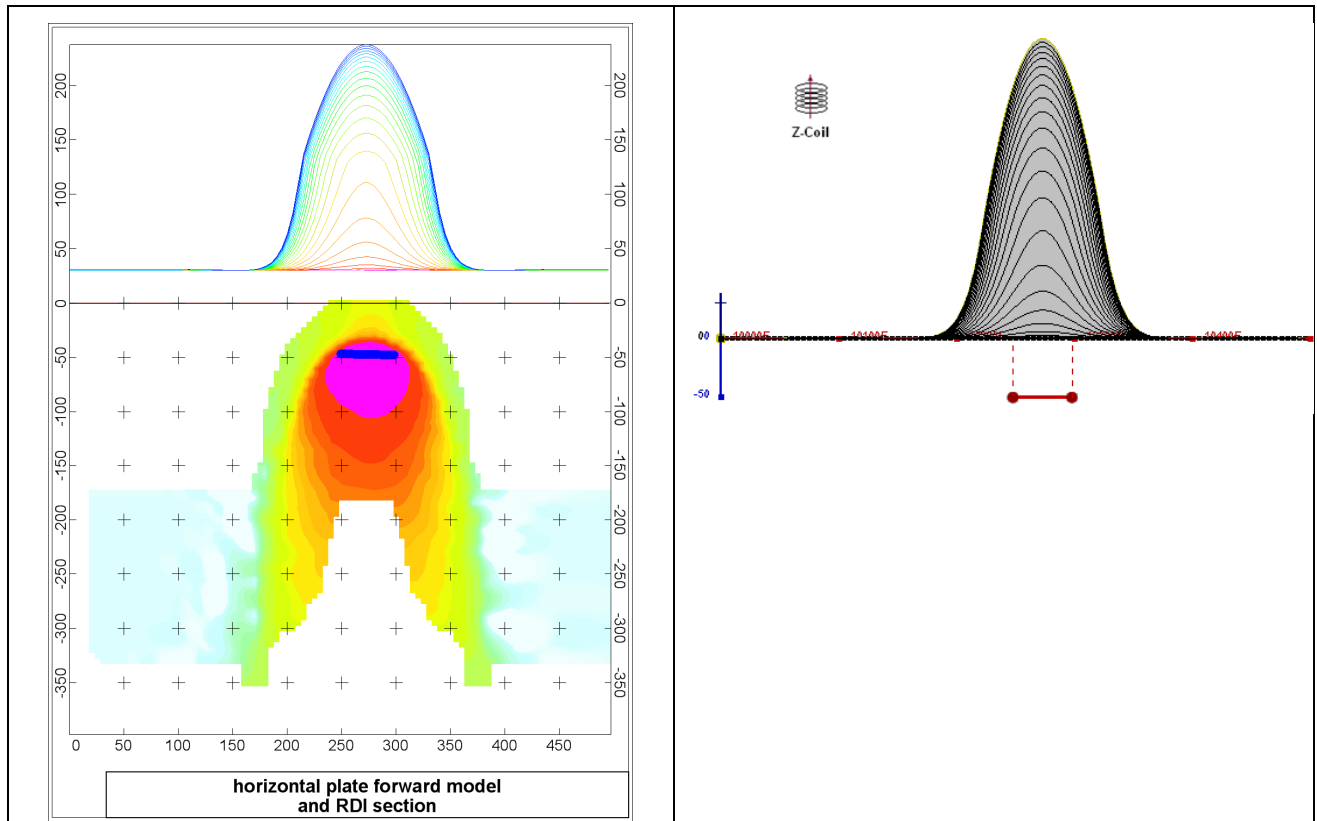


**Figure F-5:** Maxwell plate model and RDI from the calculated response for horizontal thin plate (depth 50 m, dim 50x100 m). 15-44 chan.

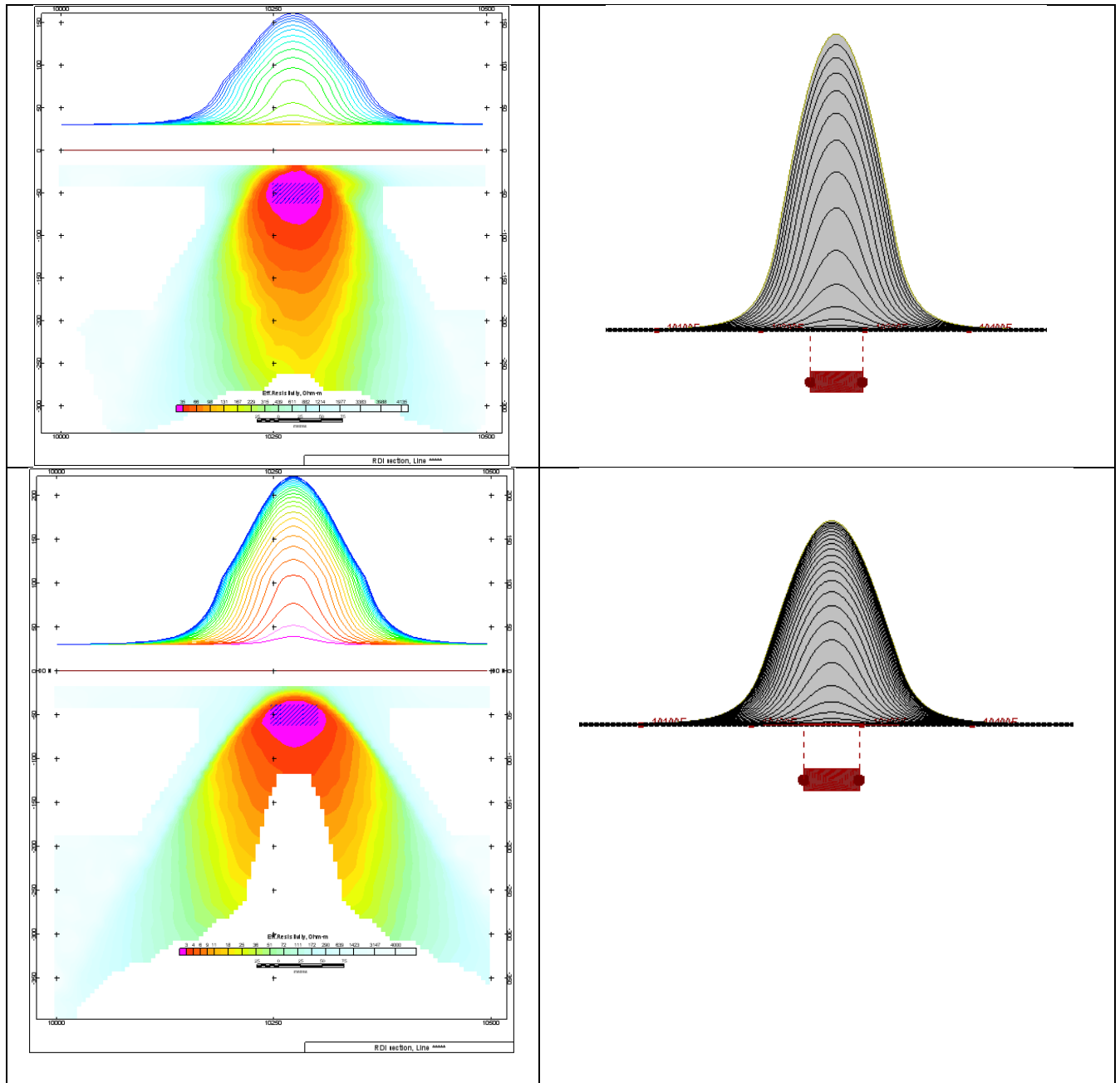


**Figure F-6:** Maxwell plate model and RDI from the calculated response for horizontal thick (20m) plate – less conductive (on the top), more conductive (below).

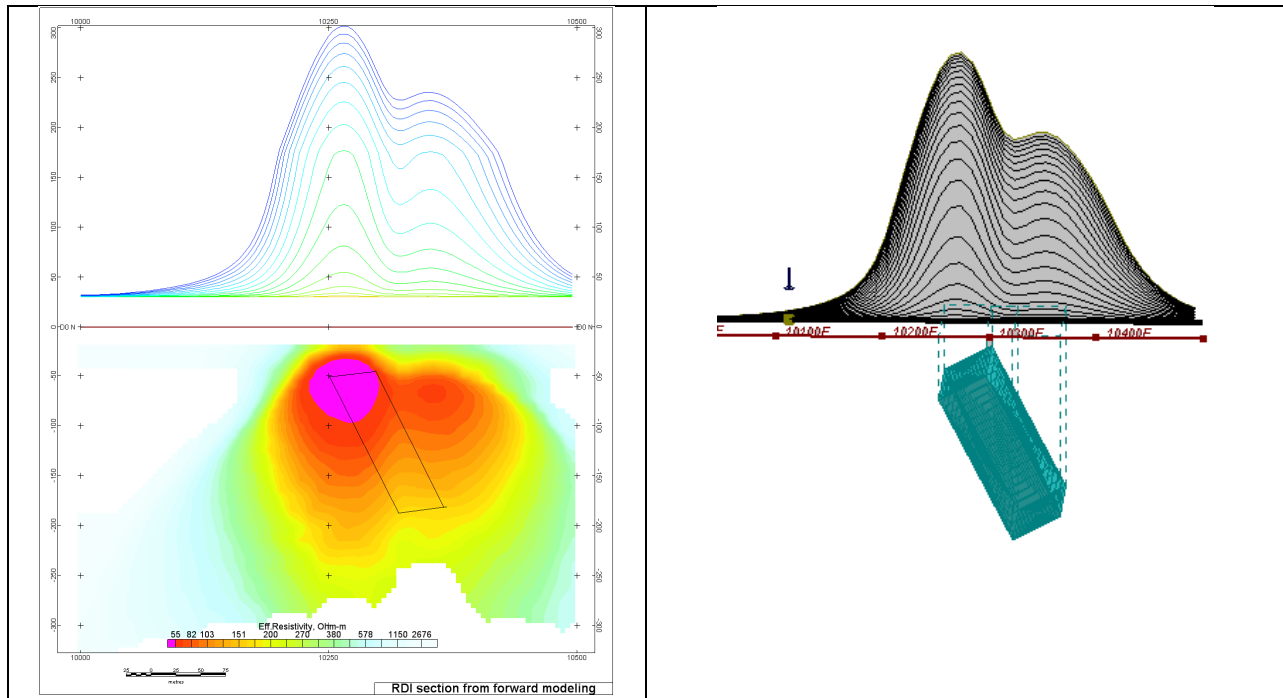


**Figure F-7:** Maxwell plate model and RDI from the calculated response for inclined thick (50m) plate. Depth extends 150 m, depth to the target 50 m.

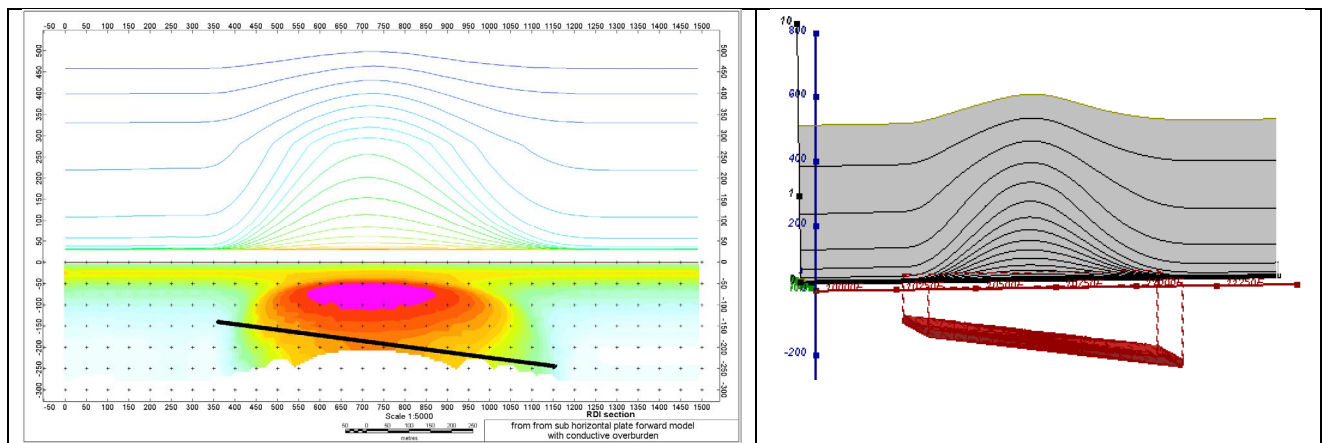


**Figure F-8:** Maxwell plate model and RDI from the calculated response for the long, wide and deep subhorizontal plate (depth 140 m, dim 25x500x800 m) with conductive overburden.

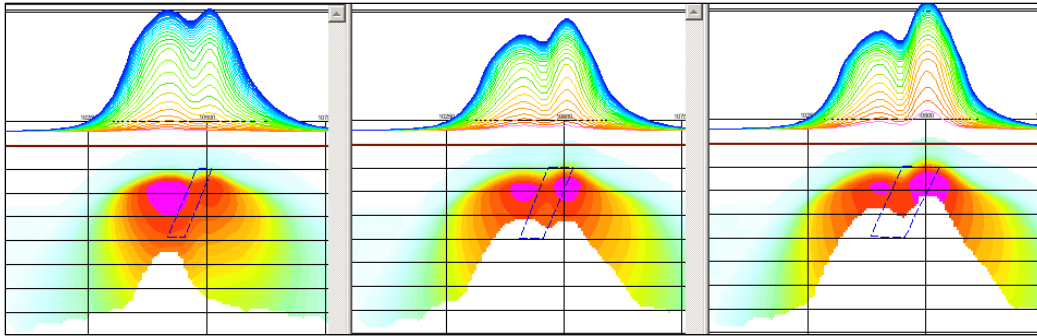


**Figure F-9:** Maxwell plate models and RDIs from the calculated response for "thick" dipping plates (35, 50, 75 m thickness), depth 50 m, conductivity 2.5 S/m.

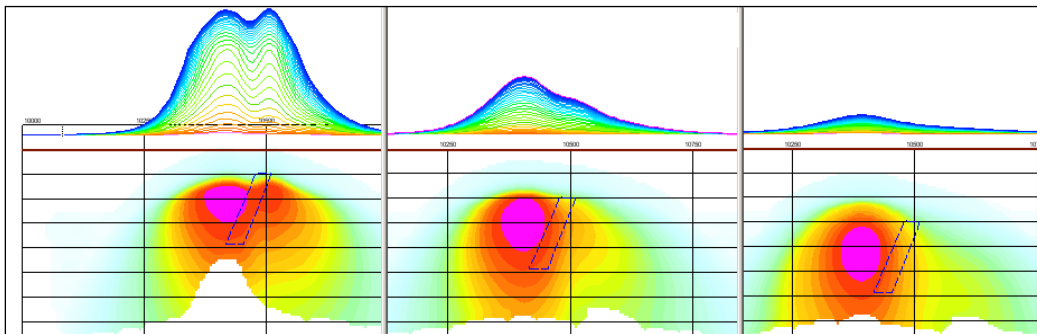


**Figure F-10:** Maxwell plate models and RDIs from the calculated response for "thick" (35 m thickness) dipping plate on different depth (50, 100, 150 m), conductivity 2.5 S/m.

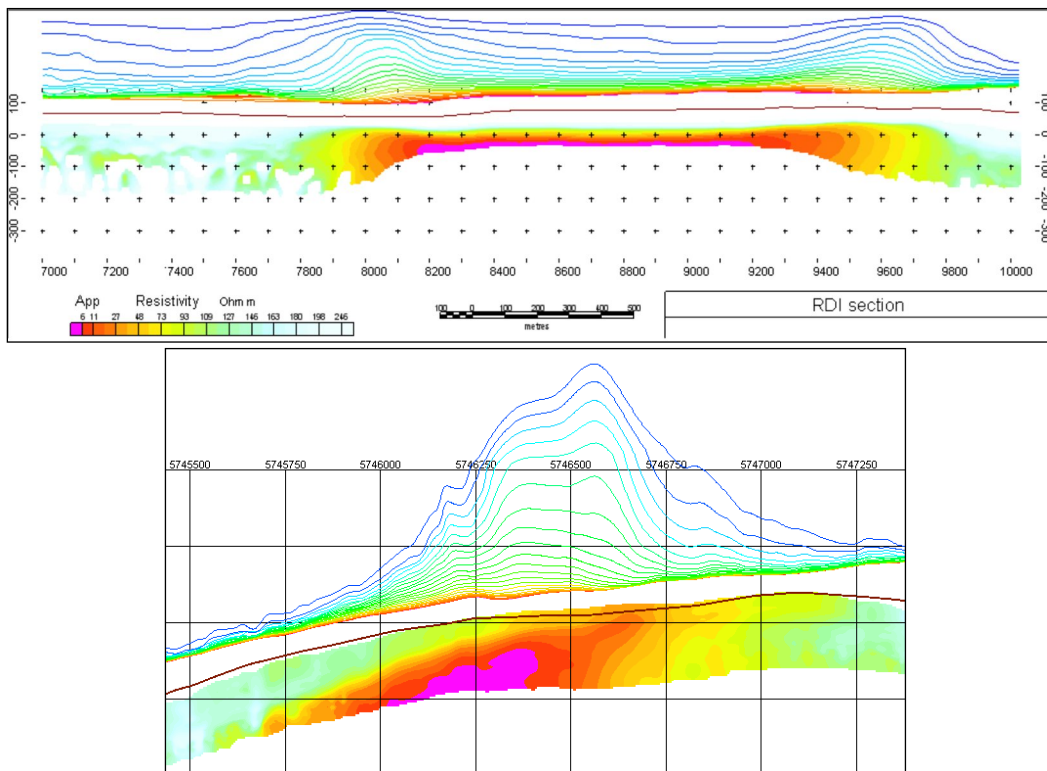
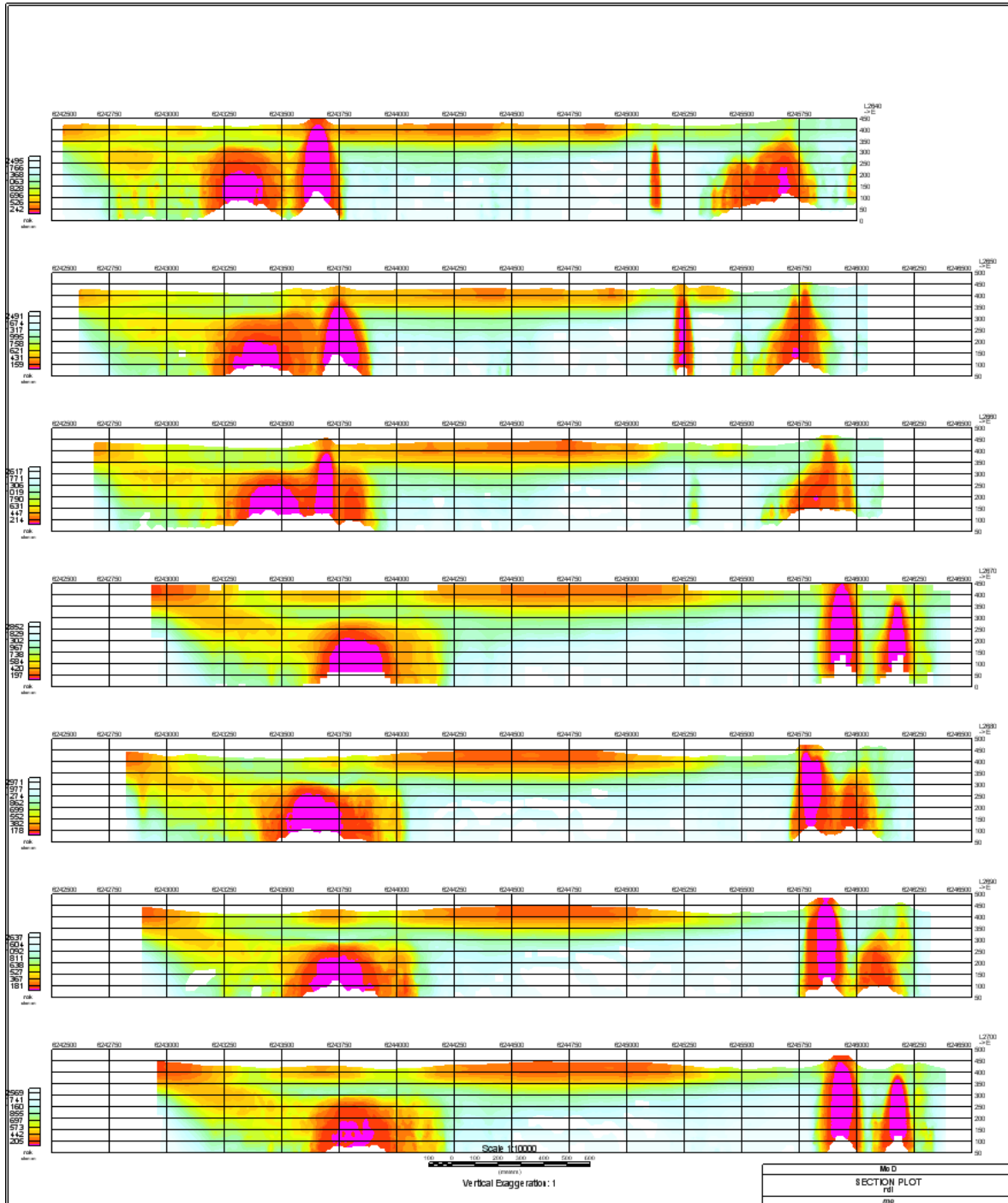


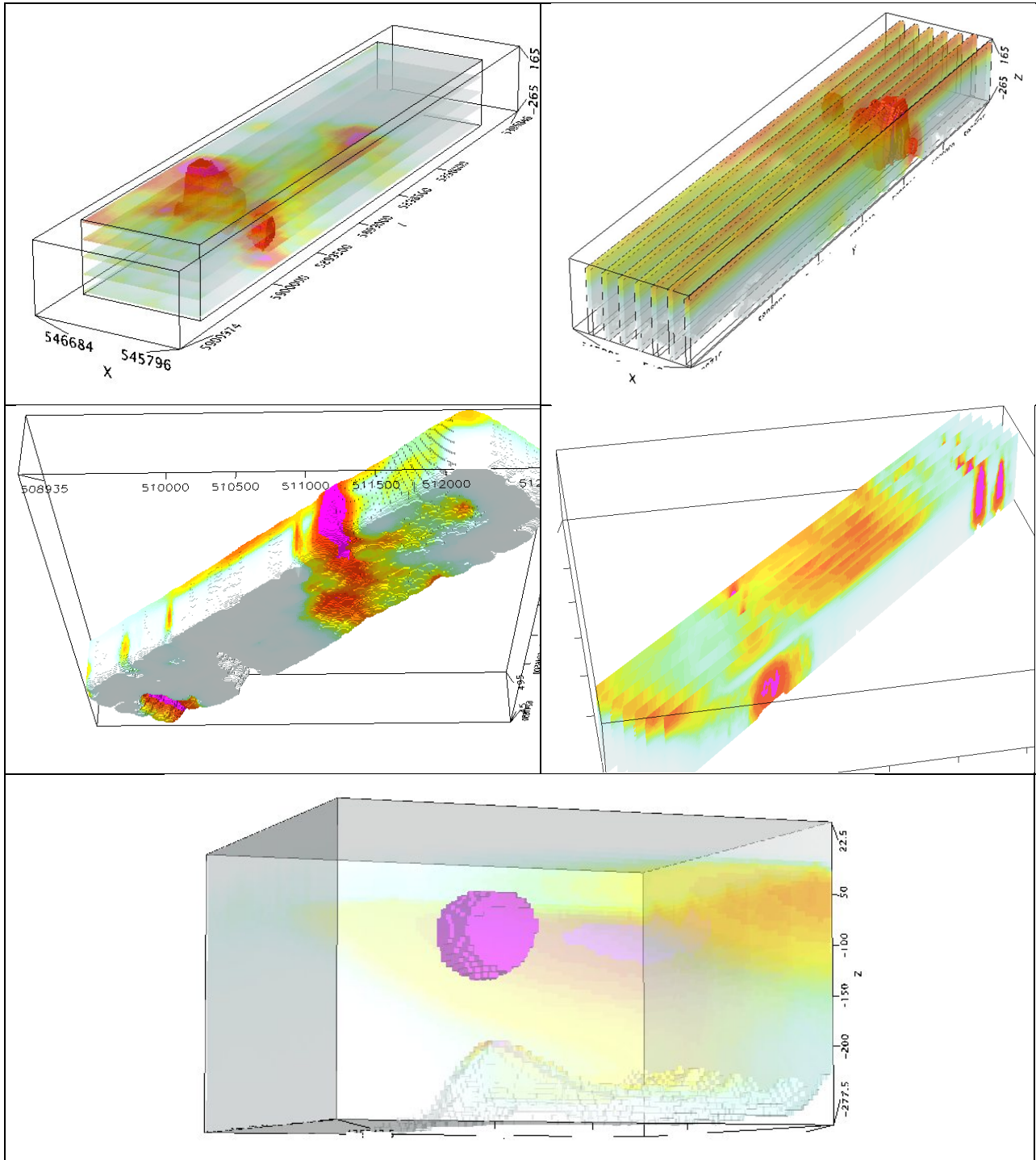
**Figure F-11:** RDI section for the real horizontal and slightly dipping conductive layers.

# FORMS OF RDI PRESENTATION

## PRESENTATION OF SERIES OF LINES

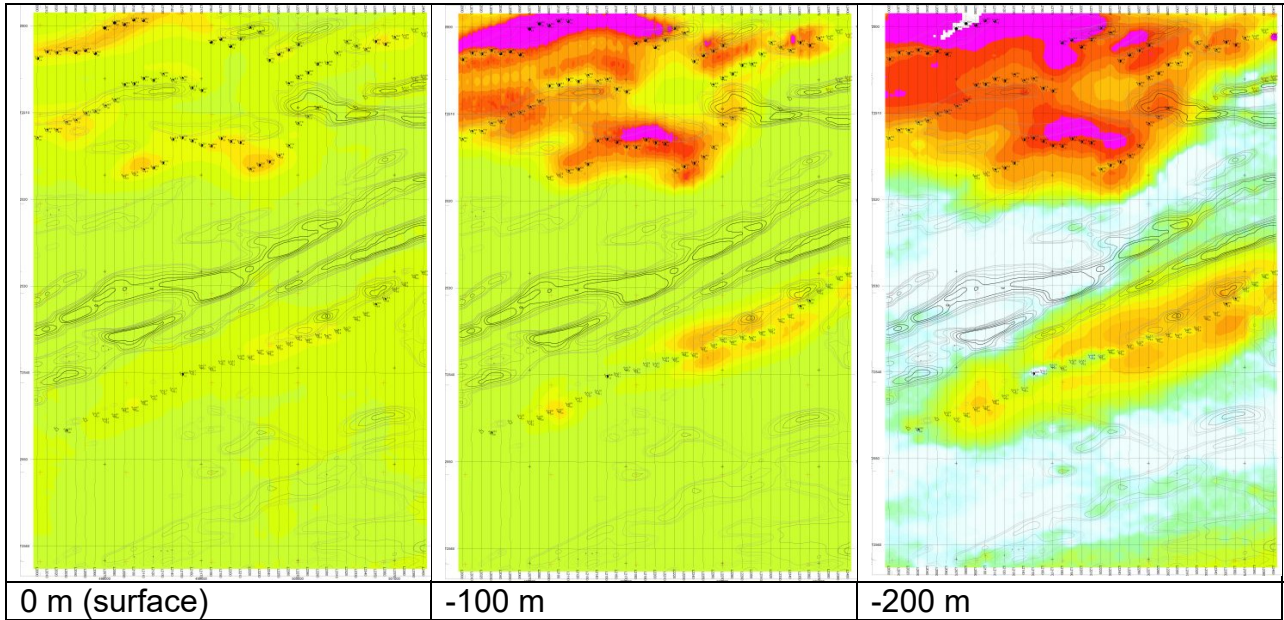


### 3D PRESENTATION OF RDIS

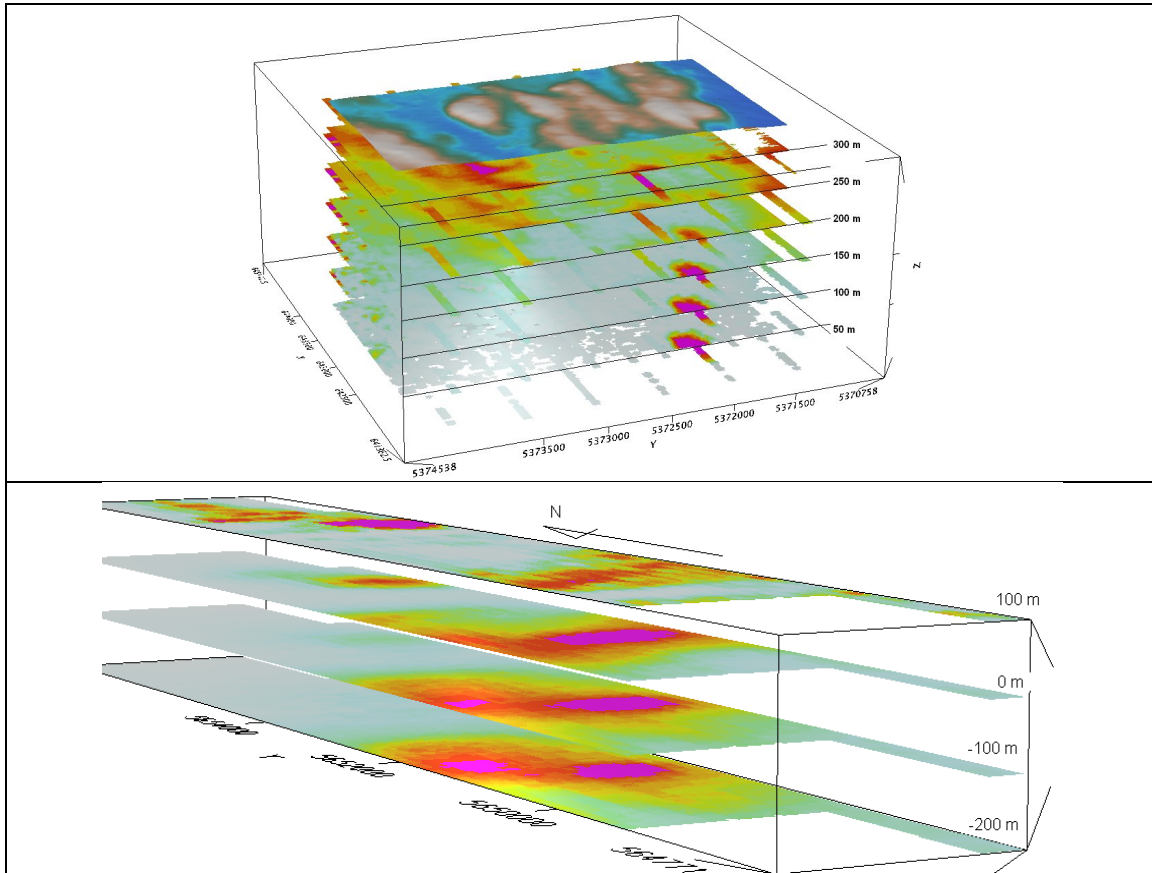




**APPARENT RESISTIVITY DEPTH SLICESPLANS:**

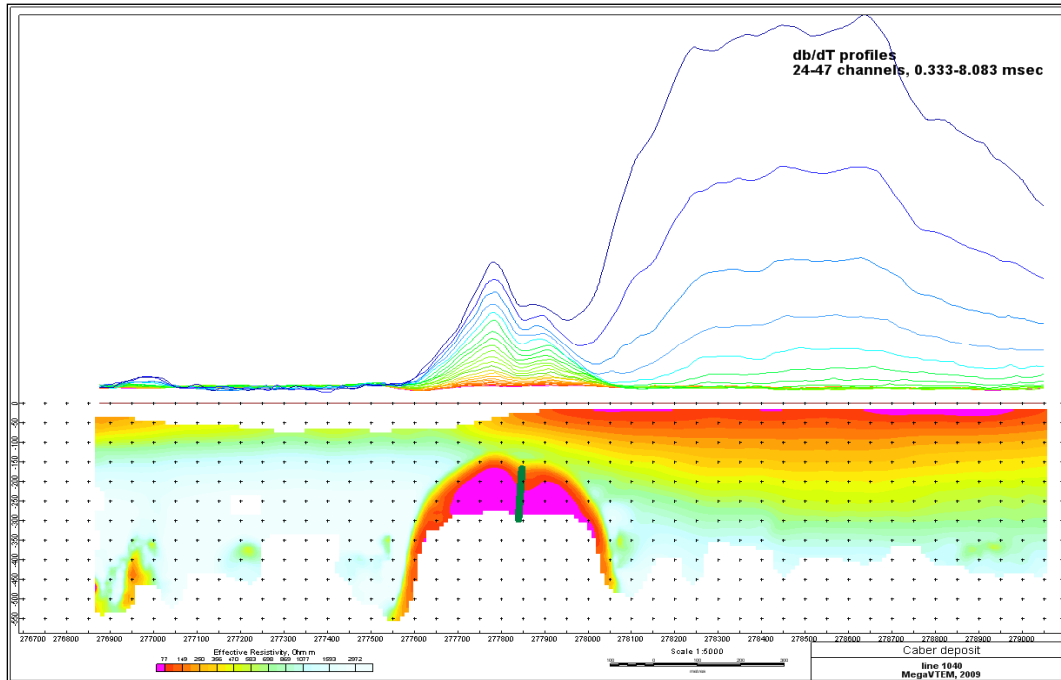


**3D VIEWS OF APPARENT RESISTIVITY DEPTH SLICES:**

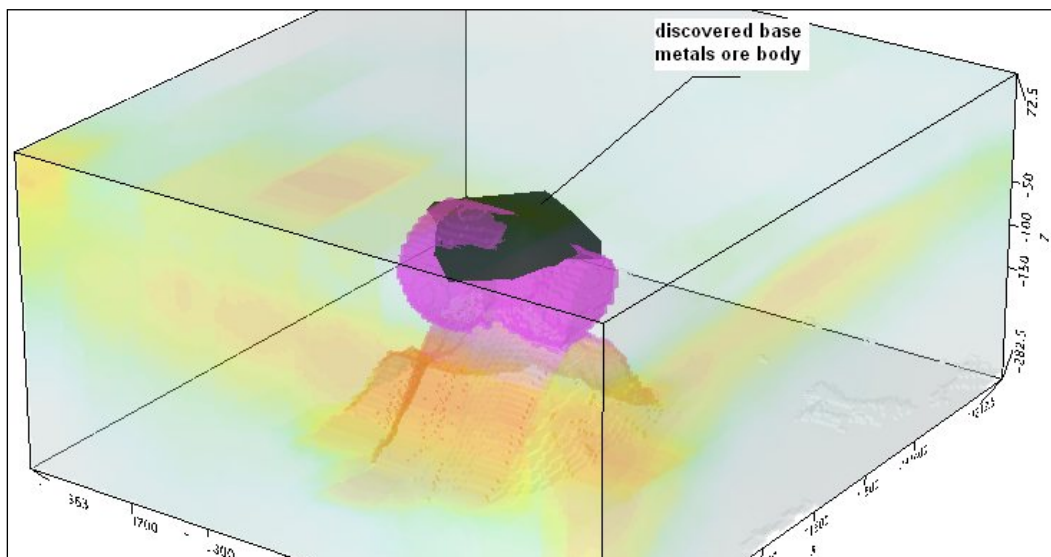


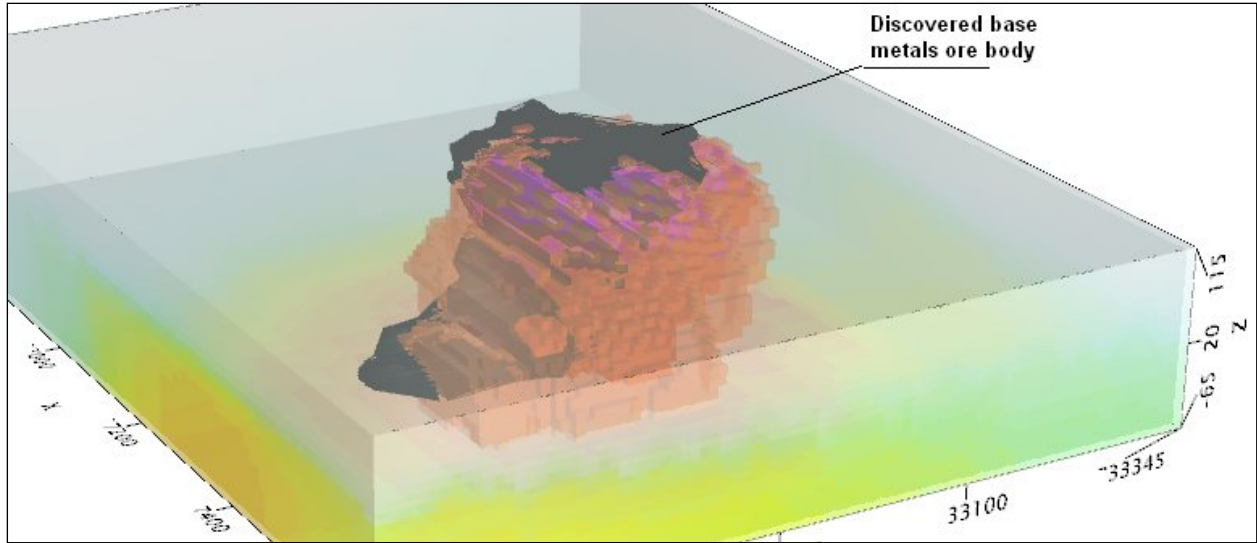
## REAL BASE METAL TARGETS IN COMPARISON WITH RDIS:

RDI section of the line over Caber deposit ("thin" subvertical plate target and conductive overburden).



## 3D RDI VOXELS WITH BASE METALS ORE BODIES (MIDDLE EAST):





**Geotech Ltd.**  
April 2011

## APPENDIX G

RESISTIVITY DEPTH IMAGES (RDI)  
Please see RDI Folder on DVD for the PDF's